


Fall 12-2016

## Structure-Property Relationships of Polyisobutylene-Block-Polyamide Thermoplastic Elastomers

Morgan Dunn Heskett  
*University of Southern Mississippi*

Follow this and additional works at: [https://aquila.usm.edu/masters\\_theses](https://aquila.usm.edu/masters_theses)

 Part of the [Other Engineering Science and Materials Commons](#), [Polymer and Organic Materials Commons](#), and the [Polymer Chemistry Commons](#)

---

### Recommended Citation

Heskett, Morgan Dunn, "Structure-Property Relationships of Polyisobutylene-Block-Polyamide Thermoplastic Elastomers" (2016). *Master's Theses*. 267.  
[https://aquila.usm.edu/masters\\_theses/267](https://aquila.usm.edu/masters_theses/267)

This Masters Thesis is brought to you for free and open access by The Aquila Digital Community. It has been accepted for inclusion in Master's Theses by an authorized administrator of The Aquila Digital Community. For more information, please contact [Joshua.Cromwell@usm.edu](mailto:Joshua.Cromwell@usm.edu).

STRUCTURE-PROPERTY RELATIONSHIPS OF POLYISOBUTYLENE-*BLOCK*-  
POLYAMIDE THERMOPLASTIC ELASTOMERS

by

Morgan Dunn Heskett

A Thesis  
Submitted to the Graduate School  
and the School of Polymers and High Performance Materials  
at The University of Southern Mississippi  
in Partial Fulfillment of the Requirements  
for the Degree of Master of Science

Approved:

---

Dr. Robson Storey, Committee Chair  
Professor, Polymers and High Performance Materials

---

Dr. Derek Patton, Committee Member  
Associate Professor, Polymers and High Performance Materials

---

Dr. Jeffrey Wiggins, Committee Member  
Associate Professor, Polymers and High Performance Materials

---

Dr. Karen S. Coats  
Dean of the Graduate School

December 2016

COPYRIGHT BY

Morgan Dunn Heskett

2016

*Published by the Graduate School*



## ABSTRACT

### STRUCTURE-PROPERTY RELATIONSHIPS OF POLYISOBUTYLENE-BLOCK-POLYAMIDE THERMOPLASTIC ELASTOMERS

by Morgan Dunn Heskett

December 2016

Thermoplastic elastomers (TPEs) are a class of polymer fit for a wide variety of applications due to their customizability. In the synthesis of these types of materials, an elastically-performing polymer, deemed the “soft block,” is combined with a stiffer “hard block” polymer, each of which can be selected based on their own specific properties in order to achieve desired material behavior in the final copolymer. Recently, the use of polyisobutylene as a soft block in combination with a polyamide hard block has been investigated for use in TPE synthesis. While the material showed some promising behavior, many properties were still below those of the commercially standard TPE material Pebax<sup>®</sup>.

Polyisobutylene and polyamide samples of varying molecular weights and types were synthesized and combined in different ratios to form a variety of polyisobutylene-*block*-polyamide (PIB-PA) samples. Mechanical stirring as opposed to magnetic mixing and an increase in the soft block component of the copolymer were the most important adjustments made from previous PIB-PA syntheses. The effect of overall block length and the incorporation of a wider variety of polyamide (PA) types were also investigated.

Mechanical stirring allowed for the achievement of higher molecular weights, and use of PA-6,6 as a hard block also produced a TPE with a markedly higher melting point than previously witnessed. Increasing the PIB content as well as using longer blocks of

both precursors produced tougher copolymers, allowing them to undergo more mechanical deformation before failure as compared to previous PIB-PA formulations.

## ACKNOWLEDGMENTS

I'd first like to thank my advisor, Dr. Robson Storey, for taking a chance on welcoming an engineer into his synthesis-heavy research group. Under his tutelage not only did I gain an increase in organic chemistry knowledge, but also development in working in a professional scientific environment.

I would also like to recognize the rest of the faculty and staff in the School of Polymers and High Performance Materials for all of their assistance and guidance during my time at Southern Miss, especially my committee members, Dr. Derek Patton and Dr. Jeffrey Wiggins. Several other people deserve special recognition for their contribution to the work presented in the following pages, including Dr. William Jarrett, Dr. Heather Broadhead, and Richard Ferguson for all of their instrumentation knowledge and assistance. I'd also like to thank Melanie Heusser and Bret Calhoun, who I could always count on to solve any administrative problems I encountered.

Additionally, my colleagues in the Storey Research Group were vital in completing this work. The first recognition goes to Dr. Lauren Kucera, who paved the way for me to work on this PIB-PA project. I'd also like to thank all the previous and current SRG members who not only contributed to my scientific advancements, but made work an enjoyable place to be: Dr. Mark Brei, Garrett Campbell, Bin Yang, Corey Parada, Hunter Cooke, Travis Holbrook, Tom Wu, and Merlin Dartez. The SRG undergraduate students who assisted in lab are also worthy of recognition, especially Sam Hanson, who specifically assisted me with initiator synthesis.

## DEDICATION

There are a lot of people who deserve thanks for making my time in Hattiesburg memorable. To the Forgotten Class of 2012-2013: thank you for helping me survive first year; I don't think I could have made it to this point without all of your assistance. To my fellow DDDR and Tuesday Night Trivia members: thanks for providing me with some (mostly) non-polymer entertainment to help even out the "life" side of work-life balance. To Kat, Christina, Ashleigh, Katelyn, and especially Brooks and Emily: thanks for housing me during the final stretch; I literally, physically could not have been here to complete this work without your generosity.

And lastly, but certainly not least, I would like to thank my family for supporting me throughout this experience. Minnie, for quelling my crazy cat lady needs. The Heskett Huddle, for their constant support over the last few years, no matter how far across the country we spread. My brother Shane, for reminding me that "grad school normal" isn't necessarily "real life normal." And, most of all, my parents, for many reasons—but mostly for the hours they've listened to me vent on the phone, for the months of cat-sitting, and for always encouraging me when I needed it the most.

## TABLE OF CONTENTS

ABSTRACT .....	ii
ACKNOWLEDGMENTS .....	iv
DEDICATION .....	v
LIST OF TABLES .....	ix
LIST OF ILLUSTRATIONS .....	x
LIST OF SCHEMES.....	xiii
LIST OF ABBREVIATIONS.....	xiv
CHAPTER I - INTRODUCTION .....	1
CHAPTER II – SYNTHESIS AND CHARACTERIZATION OF POLYISOBUTYLENE, POLYAMIDE, AND POLYISOBUTYLENE- <i>BLOCK</i> - POLYAMIDE COPOLYMERS .....	10
2.1 Introduction.....	10
2.2 Experimental .....	11
2.2.1 Materials .....	11
2.2.2 Instrumentation .....	12
2.2.3 Synthesis and characterization of polyisobutylenes .....	13
2.2.3.1 Synthesis of $\alpha,\omega$ -bis[4-(3-bromopropoxy) phenyl]polyisobutylene .....	13
2.2.3.2 Synthesis of $\alpha,\omega$ -bis[4-(3-phthalimidopropoxy)phenyl] polyisobutylene .....	15
2.2.3.3 Synthesis of $\alpha,\omega$ -bis[4-(3-aminopropoxy)phenyl] polyisobutylene .....	15



2.2.3.4 Characterization of polyisobutylenes.....	16
2.2.4 Synthesis and characterization of polyamides .....	18
2.2.4.1 Synthesis of polyamides .....	18
2.2.4.2 Trifluoroacetylation of polyamides for GPC characterization.....	20
2.2.4.3 Titration of polyamides for molecular weight determination .....	20
2.2.4.4 MALDI-TOF MS of polyamides .....	21
2.2.5 Synthesis of polyisobutylene- <i>block</i> -polyamide copolymers .....	22
2.2.5.1 Design of Experiments (DOE).....	23
2.2.5.1.1 Experimental .....	24
2.2.5.1.2 Results.....	25
2.2.5.2 Extended time PIB-PA copolymerization.....	28
2.2.5.3 Ladder study.....	31
2.2.5.3.1 Experimental .....	32
2.2.5.3.2 Results.....	33
 CHAPTER III – MECHANICAL AND THERMAL PROPERTIES OF POLYISOBUTYLENE- <i>BLOCK</i> -POLYAMIDE THERMOPLASTIC ELASTOMERS	
3.1 Experimental.....	36
3.1.1 Materials .....	36
3.1.2 Instrumentation .....	36
3.2 Results.....	39

3.2.1 Thermogravimetric Analysis (TGA).....	40
3.2.2 Differential Scanning Calorimetry (DSC) .....	44
3.2.3 Dynamic Mechanical Analysis (DMA) .....	48
3.2.4 Tensile Testing.....	58
3.3 Conclusions.....	66
APPENDIX A – Supplementary Figures and Tables .....	68
REFERENCES .....	70

## LIST OF TABLES

Table 2.1 Polyamide formulations and yields.....	19
Table 2.2 Polyamide molecular weights as determined by GPC, titration, and MALDI-TOF MS .....	20
Table 2.3 Design of Experiments molecular weight results .....	25
Table 2.4 ANOVA Calculated p-values .....	26
Table 2.5 Molecular weights of PIB-PA samples from extended copolymerizations.....	29
Table 2.6 Mechanical stirring ladder study molar ratios and resultant molecular weights .....	33
Table 3.1 TGA degradation temperatures for PIB-PA and Pebax <sup>®</sup> TPEs .....	42
Table 3.2 DSC data for PIB-PA 11 samples with varying weight ratios.....	45
Table 3.3 Notable DSC transition temperatures for 3:1 PIB-PA samples.....	47
Table 3.4 Mechanical properties of PIB-PA 11 samples with varying weight ratios.....	59
Table 3.5 Mechanical properties of 3:1 PIB-PA 11 samples with varying block lengths	61
Table 3.6 Mechanical properties of 3:1 PIB-PA and Pebax <sup>®</sup> TPEs .....	63
Table 3.7 Tension set results for PIB-PA and Pebax <sup>®</sup> TPEs .....	65
Table A.1 Polyamide MALDI-TOF MS molecular weight experimental and theoretical comparison.....	69

## LIST OF ILLUSTRATIONS

Figure 1.1 Structure of Upjohn Company's polyester-amide TPE.....	2
Figure 1.2 Comparison of soft block repeat units.....	8
Figure 1.3 Kucera's ladder study of 2:2 PIB-PA 11.....	9
Figure 2.1 <sup>1</sup> H-NMR spectra of (A) $\alpha,\omega$ -bis[4-(3-bromopropoxy)phenyl]polyisobutylene, (B) $\alpha,\omega$ -bis[4-(3-phthalimidopropoxy)phenyl]polyisobutylene, and (C) $\alpha,\omega$ -bis[4-(3- aminopropoxy)phenyl]polyisobutylene. ....	17
Figure 2.2 MALDI-TOF MS spectrum for PA-11.....	22
Figure 2.3 Design of Experiments molecular weight interval plots. ....	27
Figure 2.4 Molecular weights of PIB-PA samples from extended copolymerizations.....	30
Figure 2.5 GPC light scattering traces of 48 h copolymerization aliquots. ....	31
Figure 2.6 Mechanical stirring ladder study molecular weights.....	34
Figure 3.1 TGA thermogram of starting materials (PIB and PA-11) and resulting copolymer. ....	40
Figure 3.2 TGA thermogram comparison of PIB-PA 11 samples with varying weight ratios.....	41
Figure 3.3 TGA thermogram comparison of 3:1 PIB-PA samples.....	42
Figure 3.4 TGA thermogram comparison of Pebax <sup>®</sup> and representative PIB-PA TPEs..	43
Figure 3.5 DSC thermogram comparison of PIB-PA 11 samples with varying weight ratios.....	44
Figure 3.6 DSC thermogram comparison of 3:1 PIB-PA 11 samples with varying block lengths. ....	46
Figure 3.7 DSC thermogram comparison of 3:1 PIB-PA samples. ....	47

Figure 3.8 DMA temperature ramp of PIB-PA 11 samples with varying weight ratios. .	49
Figure 3.9 DMA temperature ramp of 3:1 PIB-PA 11 samples with varying block lengths. .....	51
Figure 3.10 DMA temperature ramp of 3:1 PIB-PA samples. ....	52
Figure 3.11 DMA temperature ramp of Pebax <sup>®</sup> and representative PIB-PA TPEs.....	53
Figure 3.12 DMA room temperature frequency sweep of PIB-PA 11 samples with varying weight ratios.....	54
Figure 3.13 DMA room temperature frequency sweep of 3:1 PIB-PA 11 samples with varying block lengths.....	55
Figure 3.14 DMA room temperature frequency sweep of 3:1 PIB-PA samples. ....	56
Figure 3.15 DMA room temperature frequency sweep of Pebax <sup>®</sup> and representative PIB- PA TPEs.....	57
Figure 3.16 DMA frequency sweep-temperature step comparison of PEBAX 35 and PIB- PA 12. ....	58
Figure 3.17 Representative stress-strain curves for PIB-PA 11 samples with varying weight ratios.....	59
Figure 3.18 Representative stress-strain curves for 3:1 PIB-PA 11 samples with varying block lengths. ....	61
Figure 3.19 Representative stress-strain curves for 3:1 PIB-PA samples. ....	62
Figure 3.20 Representative stress-strain curves of Pebax <sup>®</sup> and representative PIB-PA TPEs.....	64
Figure A.1 MALDI-TOF MS spectrum for PA-12.....	68
Figure A.2 MALDI-TOF MS spectrum for PA-6.....	68

Figure A.3 MALDI-TOF MS spectrum for PA-6,6..... 69

## LIST OF SCHEMES

Scheme 1.1 Representative synthesis of Atochem's polyamide-based TPE. ....	3
Scheme 1.2 Representative synthesis of PIB-PA copolymer by Kennedy utilizing one- prepolymer method. ....	5
Scheme 1.3 Representative synthesis of PIB-PA 11 by Kucera. ....	6

## LIST OF ABBREVIATIONS

<i>TPE</i>	Thermoplastic elastomer
<i>PA</i>	Polyamide
<i>PTMO</i>	Poly(tetramethylene oxide)
<i>PPO</i>	Poly(propylene oxide)
<i>PIB</i>	Polyisobutylene
$T_g$	Glass transition temperature
<i>SIBS</i>	Polystyrene-polyisobutylene-polystyrene
<i><math>\alpha</math>MeSt</i>	$\alpha$ -Methylstyrene
<i>PIB-PA</i>	Polyisobutylene- <i>block</i> -polyamide
<i>PEO</i>	Polyethylene oxide
<i>TiCl<sub>4</sub></i>	Titanium(IV) chloride
<i>MgSO<sub>4</sub></i>	Magnesium sulfate
<i>NMP</i>	<i>N</i> -methyl-2-pyrrolidone
<i>AA</i>	Adipic acid
<i>12-ADA</i>	12-Aminoundecanoic acid
<i>HMD</i>	1,6-Hexanediamine
<i>THF</i>	Tetrahydrofuran
<i>11-AUA</i>	11-Aminoundecanoic acid
<i><math>\epsilon</math>-CAP</i>	$\epsilon$ -Caprolactam
<i>6-ACA</i>	6-Aminocaproic acid
<i>DCM</i>	Dichloromethane
<i>TFAA</i>	Trifluoroacetic anhydride



<i>bDCC</i>	5- <i>tert</i> -Butyl-1,3-bis(1-chloro-1-methylethyl)benzene
<i>NMR</i>	Nuclear magnetic resonance
<i>TMS</i>	Tetramethylsilane
$M_n$	Number-average molecular weight
<i>PDI</i>	Polydispersity index
<i>GPC</i>	Gel permeation chromatography
<i>MALS</i>	Multi-angle light scattering
<i>dRI</i>	Differential refractive index
<i>dn/dc</i>	Refractive index increment
<i>ATR-FTIR</i>	Attenuated total reflectance Fourier transform infrared
<i>MALDI-TOF MS</i>	Matrix-assisted laser desorption ionization time-of-flight mass spectroscopy
<i>DOE</i>	Design of Experiments
<i>ANOVA</i>	Analysis of variance
<i>TGA</i>	Thermogravimetric analysis
$T_{di}$	Degradation temperature (initial)
$T_{dm}$	Degradation temperature (maximum)
<i>DSC</i>	Differential scanning calorimetry
$T_m$	Melting temperature
$T_c$	Crystallization temperature
<i>DMA</i>	Dynamic mechanical analysis

*EMTS*

Electromechanical testing system

*AFM*

Atomic force microscopy

## CHAPTER I - INTRODUCTION

Thermoplastic elastomers (TPEs) are materials that display the processability of traditional thermoplastics while also providing certain desirable properties of elastomeric materials, especially the recoverable elasticity found in materials such as vulcanized rubbers. This combination of advantageous properties is made possible by the structure of TPEs, which typically consist of two different components: a hard block material, providing the TPE's strength and resistance to irreversible deformation, and a soft block material, responsible for the elastomeric behavior of the product. The ability to choose from a variety of polymers for the hard and soft block of TPEs enables them to be very customizable materials, allowing the user to fine-tune the properties desired in the final product.

The material that could be considered the first thermoplastic elastomer was a polyester fiber produced by melt copolymerization of a dicarboxylic acid and a glycol, patented by DuPont in 1952. The defining characteristic of this material was its ability to display at least 90% elastic recovery within just one minute following an elongation of 100%.<sup>1</sup> Over the next couple of decades, the TPE field grew rapidly as different polymers were utilized in TPE formulations—for example, styrene-diene block copolymers, thermoplastic polyolefin blends, and thermoplastic vulcanizates all emerged by the 1970s.<sup>2</sup>

By the late 1970s, polyamide-based TPEs emerged onto the market. The Upjohn Company (now a part of Dow Chemical) introduced polyester-amides onto the market which were processable by injection molding, qualifying them to be defined as TPEs, a feat previously unachieved by other polyester-amides that were unable to withstand the

high temperatures needed to perform in TPE applications while maintaining a low enough melt temperature to be easily processed.<sup>3</sup> The material, a general structure of which is given in Figure 1.1, was produced using a one-prepolymer method: a dicarboxylic acid is first reacted with a diol to form a polyester prepolymer (soft block), which is then reacted with a diisocyanate to form the hard blocks *in situ*.

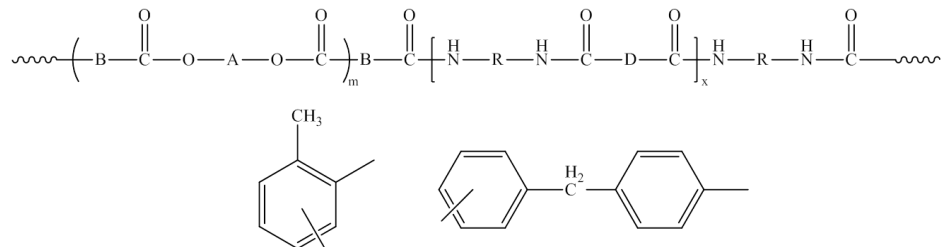
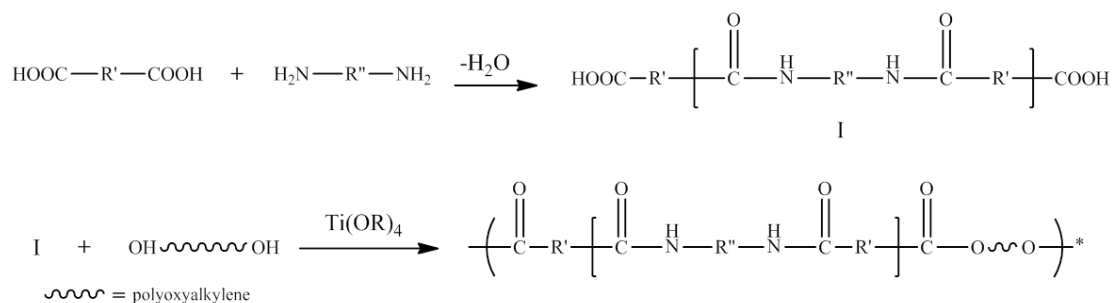


Figure 1.1 Structure of Upjohn Company's polyester-amide TPE.

In the upper structure, A represents the residue of a diol with molecular weight in the range of 400-4,000 g/mol, B is the residue of an aliphatic dicarboxylic acid with 6-14 carbon atoms, D is the residue of a carboxylic acid (chosen so as not to raise the melting temperature of the hard block to a value above 280-300 °C), and R is an arylene chosen from the two structures provided in the lower half of the figure. The average value of m falls between 0 and 1, and the average value of x falls between 0 and 10.

In 1982, Atochem introduced a polyether-ester-amide which met the previously given qualifications needed to be considered a TPE. The material was a block copolymer produced by a two-prepolymer method: polycondensation of a dicarboxylic acid-terminated polyamide (PA) hard block and a dihydroxyl-terminated polyether soft block, as seen in Scheme 1.1. The resulting material was processable by extrusion and displayed “outstanding mechanical properties.”<sup>4</sup>



Scheme 1.1 Representative synthesis of Atochem's polyamide-based TPE.

R' is an aliphatic chain consisting of 4 to 10 carbon atoms, and R'' is an aliphatic chain consisting of 6 to 9 carbon atoms. Ti(OR)<sub>4</sub> is a tetraalkylorthotitanate catalyst where R is a linear, branched aliphatic carbon chain comprised of 1 to 24 carbon atoms.

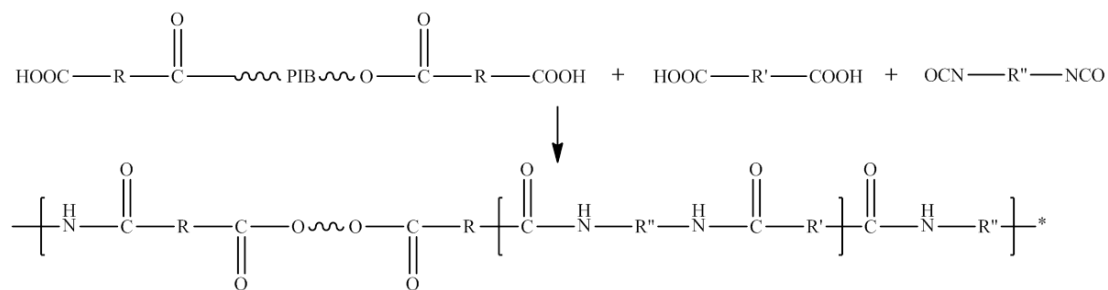
Mechanical properties of the early Atochem materials were tunable to desired levels by variation of the prepolymers chosen as starting materials: for example, implementing different molecular weight ratios between the hard and soft blocks introduced various levels of elasticity in the final copolymer.<sup>4</sup> This made the material, later named Pebax<sup>®</sup>, applicable to a wide variety of industrial applications. In the years since, more polyamide-based TPEs have entered the market: for example, Evonik's VESTAMID<sup>®</sup> E material which combines a PA hard block with a poly(tetramethylene oxide) (PTMO) soft block, and Ube's PAE, which utilizes poly(propylene oxide) (PPO) as a soft block.<sup>5</sup>

Generally, commercial polyamide-based TPEs utilize polyether as a soft block. However, polyisobutylene (PIB) as a soft block material has been reported in literature as well. Due to its fully saturated hydrocarbon backbone, PIB is inert and highly resistant to degradation, especially by oxygen and ozone.<sup>6</sup> The low glass transition temperature (T<sub>g</sub>) of PIB, measuring in the range of -73 to -65 °C dependent upon molecular weight,<sup>7</sup> provides it with strong low temperature properties. There are also many end group chemistries available to PIB,<sup>8</sup> meaning there are a wide variety of reactions available to

create different linkages between the PIB and the chosen hard block material in a TPE application.

Kennedy et al. used PIB as the soft block material in the synthesis of polystyrene-polyisobutylene-polystyrene (SIBS) copolymer TPEs. In the earliest syntheses of these materials, difunctional tert-chloride PIB was synthesized via the inifer method before undergoing reaction with  $\alpha$ -methylstyrene ( $\alpha$ MeSt), which added to either end of the PIB to form the anchoring hard blocks of the triblock copolymer.<sup>9</sup> However, these initial attempts at synthesis of TPEs utilizing PIB yielded materials displaying poor mechanical properties due to their inhomogeneous nature and contamination by diblock material.<sup>10</sup> Synthesis of PIB-based triblock TPEs continued to be improved upon, and additives were discovered that allowed block length to be more controlled during creation: for example, the inclusion of an electron pair donor and a proton trap allowed for the synthesis of a SIBS triblock copolymer by sequential monomer addition that successfully displayed TPE-quality mechanical properties.<sup>11</sup> SIBS copolymers have since found success as commercial materials: the year 2004 saw the introduction of SIBSTAR<sup>™</sup> by Kaneka, as well as Oppanol<sup>®</sup> IBS by BASF.<sup>12</sup>

Polyamide was first used as the hard block in TPE copolymer synthesis with a PIB soft block by Kennedy and Zschke.<sup>13</sup> The anticipated miscibility of nonpolar PIB and polar PA prompted the authors to carry out the copolymerization in a cosolvent system capable of dissolving both blocks simultaneously. The authors utilized a one-prepolymer method by reacting difunctional PIB carrying either carboxyl or isocyanate end groups with various diisocyanate/dicarboxylic acid monomer systems to form the hard PA block *in situ*. A representative reaction is shown in Scheme 1.2.

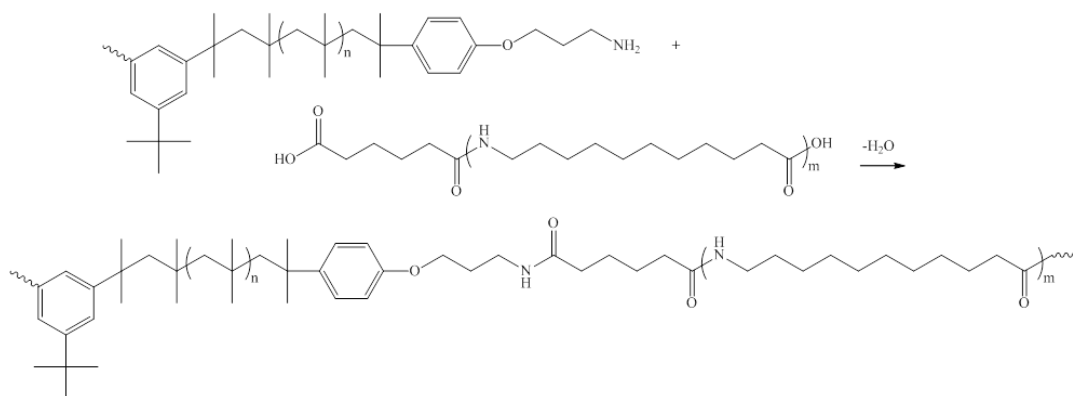


Scheme 1.2 Representative synthesis of PIB-PA copolymer by Kennedy utilizing one-prepolymer method.

In this example, difunctional carboxylic acid-terminated PIB was reacted with dicarboxylic and diisocyanate monomers; the authors also investigated the use of difunctional isocyanate-terminated PIB with the dicarboxylic/diisocyanate monomer system.

While high melting temperatures were displayed by the final PIB-PA copolymers, the materials showed poor elongation during mechanical testing. It was predicted that these mechanical properties could be improved by utilizing PIB soft blocks of a higher molecular weight. Cross-linking present in the crude product due to a stoichiometric imbalance of carboxylic acid and isocyanate end groups also caused an increased viscosity during mixing, resulting in a lower-than-expected yield.<sup>13</sup>

Kucera et al. also synthesized PIB-PA copolymers, but instead utilized a solventless, two-prepolymer method in which difunctional amine-terminated PIB and difunctional carboxylic acid-terminated PA<sup>14</sup> were reacted neat at temperatures above the melting point of the PA prepolymer, as seen in Scheme 1.3.



**Scheme 1.3** Representative synthesis of PIB-PA 11 by Kucera.

A two-prepolymer approach was used, in which a difunctional amine-terminated PIB was combined with a difunctional carboxylic acid-terminated PA to create a PIB-PA block copolymer.

The synthesis of Pebax<sup>®</sup> involves esterification as the final pre-polymer linking reaction, and therefore requires a catalyst to achieve high conversions and high molecular weights. When tetrabutylorthotitanate was used, the authors reported 95% consumption of the polyethylene glycol monomer; however, a control reaction run in the absence of catalyst showed only 65% consumption of the glycol.<sup>4</sup> In contrast, the method of Kucera et al. involves amidation, which does not require use of a catalyst for high conversion; yields in the range of 90% were reported for copolymerizations utilizing a variety of combinations of PIB and PA types.<sup>15</sup> Kucera's process is also a bulk polycondensation, as it lacks solvent. The absence of both solvent and catalyst make this copolymerization procedure more efficient and applicable to industrial processes.

Though the PIB-PA TPE synthesized by Kucera offers several theoretical advantages when compared to the commercially standard Pebax<sup>®</sup>, there are still many improvements to be made. It was reported that PIB-PA materials in which the weight ratio of the hard block polyamide to the soft block polyisobutylene is greater than or equal to one acted like a brittle material during mechanical testing. PIB-PA 2:1 TPEs



(material in which 2,000 g/mol PIB was reacted with 1,000 g/mol PA), however, showed more elastic behavior, including improvements in properties such as elongation at break and energy at break.<sup>15</sup> It is thought that these improvements were due to the increased fraction of PIB in the copolymer, since PIB provides the material with its elastomeric character. It was reported by Arkema that Pebax<sup>®</sup> copolymers having a polyoxyalkylene glycol content in the range of 60-80% by weight displayed elastomeric properties most similar to natural rubbers.<sup>4</sup> The PIB-PA copolymers tested by Kucera covered a soft block percent-by-weight range of 33-66%. The 2:1 PIB-PA (66% soft block by weight) just barely enters the Pebax<sup>®</sup> range of ratios desirable for the most elastomeric behavior; therefore, it is thought that by increasing the ratio of the soft block in the copolymer, one could see an improvement in the elastomeric properties of the material.

Additionally, an even higher soft block weight percentage might be necessary to produce optimal elastomeric properties in PIB-PA as compared to Pebax<sup>®</sup>, as the dimethyl side chains present in PIB contribute a substantial amount of its mass (as opposed to the side chain-free polyoxyalkylene). This means that in soft blocks of these two polymers with the same molecular weight, fewer repeat units of PIB (and therefore fewer backbone atoms) are present than in the polyoxyalkylene (also known as polyethylene oxide, or PEO) sample, which then produces a longer soft block. An example of this phenomenon can be seen in Figure 1.2: both soft blocks represented display a total molecular weight of 616 g/mol, but the PEBAX block contains more repeat units and almost twice as many backbone atoms as the equivalent molecular weight PIB-PA soft block, allowing it to have a longer, potentially more flexible soft block chain that could lead to better elastic performance. Therefore, longer PIB blocks

might be needed in PIB-PA copolymers in order to reach the same the same optimal mechanical properties that Pebax<sup>®</sup> experiences when soft blocks represent 60-80% of the copolymer.

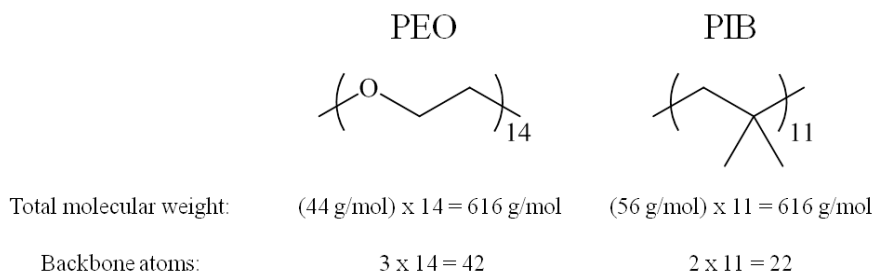


Figure 1.2 Comparison of soft block repeat units.

The repeat unit shown on the left is utilized in Pebax<sup>®</sup> materials (PEO), while the repeat unit on the right is that of PIB.

With greater focus on the weight ratio of the prepolymers used in synthesis of the PIB-PA copolymer comes the need for the most accurate data possible regarding monomer functionality values. Reaching the highest possible molecular weight for the copolymer means ensuring a high extent of reaction between the PIB and PA starting materials. The Carothers equation stipulates that for a linear polycondensation reaction of amine-terminated PIB and carboxylic acid-terminated PA, the highest extent of reaction will be achieved by reacting equimolar amounts of the amine and carboxylic acid functional groups.<sup>16</sup> Previously, it was assumed that the functionality of both the PIB and PA precursors were exactly 2, and therefore, the ratio of the two components was determined solely by the molecular weights of the materials (for example, 2 g of 2,000 g/mol PIB would be combined with 1 g of 1,000 g/mol PA to achieve a 2:1 PIB-PA material). The validity of these calculations also relies upon the assumption that the molecular weights of the PIB and PA were entirely accurate. A ladder study was carried out in order to validate these assumptions, the results of which can be seen in Figure 1.3.

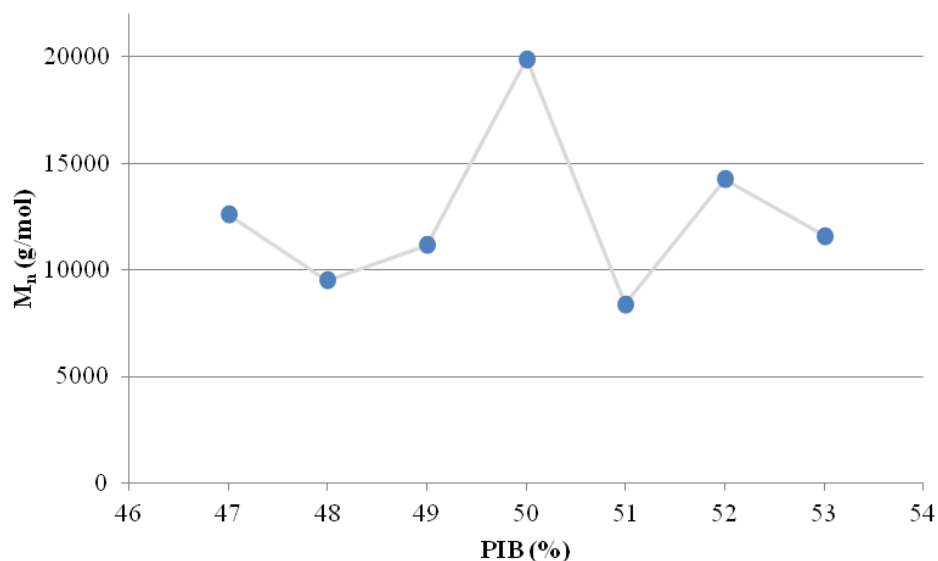


Figure 1.3 Kucera's ladder study of 2:2 PIB-PA 11.

Amounts of materials are given in weight percent, assuming a functionality of exactly 2 for each prepolymer. Materials combined were 2,000 g/mol PIB and 2,000 g/mol PA-11.

Relative amounts of PIB and PA used to achieve the desired ratios were determined by mass, assuming both prepolymers possessed the same molecular weight and functionalities of exactly 2. If this assumption is correct, the highest molecular weight would be expected to appear at the 50% PIB-50% PA data point, which is indeed the case. However, because the mass increments are spread out by 1%, it's possible that a higher molecular weight could have been reached at, for example, a 49.5% PIB-50.5% PA combination, implying that an exact functionality of 2 may not have been achieved in the synthesis of at least one of the prepolymers, or that one of the molecular weight measurements was slightly inaccurate. Therefore, a ladder study with smaller increments between data points is desired in order to attempt to more accurately determine the functionality ratio between starting materials needed to achieve the highest possible molecular weight product.

CHAPTER II – SYNTHESIS AND CHARACTERIZATION OF  
POLYISOBUTYLENE, POLYAMIDE, AND POLYISOBUTYLENE-  
*BLOCK*-POLYAMIDE COPOLYMERS

## **2.1 Introduction**

Previously, Kucera synthesized PIB-PA copolymers using a two-prepolymer method without solvent and using only magnetic stirring. Though these materials displayed some properties comparable to those of the commercial Pebax<sup>®</sup> polymers, Pebax<sup>®</sup> outperformed PIB-PAs in the areas of ultimate strain, energy, and especially elongation at break. It is known that materials with higher molecular weights show better mechanical properties; higher molecular weights allow for more entanglements between polymer chains, providing the material with improved mechanical strength.<sup>17</sup> Therefore, optimization of the molecular weight of the PIB-PA copolymers is desired. One major factor contributing to the ability of the copolymer to reach its highest potential molecular weight is accurate matching of the functionality of the prepolymers used. Difunctional prepolymers are assumed, but if the average functionality actually achieved is less than 2 for either starting material, the potential maximum molecular weight possible for the final copolymer is decreased. Therefore, one objective of this research was to optimize prepolymer synthesis methods in order to achieve as close to fully difunctional prepolymers as possible.

Optimization of the copolymerization process was another objective of the research. Previously, high viscosity of the forming material eventually prevented magnetic stirring from being an effective mixing method during PIB-PA copolymerization. Therefore, it was desired to use mechanical stirring in order to ensure

more consistent and effective mixing of the prepolymers, allowing the reaction to reach as high a conversion as possible.

## 2.2 Experimental

### 2.2.1 Materials

Hexane (anhydrous, 95%), titanium(IV) tetrachloride ( $\text{TiCl}_4$ ) (99.9%), 3-phenoxypropyl bromide (96%), magnesium sulfate ( $\text{MgSO}_4$ ) (anhydrous, 99.5%), potassium phthalimide (98%), *N*-methyl-2-pyrrolidone (NMP) (99%), ethanol (99.5%), hydrazine monohydrate ( $\text{N}_2\text{H}_4$  64-65%, reagent grade 98%), adipic acid (AA) (99.9%), 12-aminododecanoic acid (12-ADA) (95%), 1,6-hexanediamine (HMD) (99.5%), cresol red (95% dye), potassium hydroxide (85%), potassium hydrogen phthalate (99.95%), and 2,5-dihydroxybenzoic acid (98%) were purchased from Sigma-Aldrich and used as received. 2,6-Lutidine (99%), methanol (99.9%), tetrahydrofuran (THF) (99.9%), heptanes (99%), 11-aminoundecanoic acid (11-AUA) (97%),  $\epsilon$ -caprolactam ( $\epsilon$ -CAP) (99%), 6-aminocaproic acid (6-ACA) (99%), 2-propanol (99.9%), benzyl alcohol, dichloromethane (DCM) (99.9%), trifluoroacetic anhydride (TFAA) (99%), and deuterated chloroform ( $\text{CDCl}_3$ ) (99.8%, with 0.03% v/v tetramethylsilane) were purchased from Fisher Scientific and used as received. Methyl chloride (Alexander Chemical Corp.) and isobutylene (BOC Gases) were purchased from Airgas and were dried by being passed through columns of calcium sulfate, molecular sieves, and calcium chloride prior to their condensation within an  $\text{N}_2$ -atmosphere glovebox for usage. 5-*tert*-Butyl-1,3-bis(1-chloro-1-methylethyl)benzene (bDCC) was synthesized as previously reported.<sup>18</sup>

### 2.2.2 Instrumentation

Nuclear magnetic resonance (NMR) proton ( $^1\text{H}$ ) spectra were collected using a 300 MHz Varian Mercury NMR spectrometer. A standard  $^1\text{H}$  pulse sequence was used (utilizing 32 scans with a relaxation delay of 10 s) and the resulting chemical shifts were referenced to tetramethylsilane (TMS) at 0 ppm. Polyisobutylene samples were prepared for NMR characterization by dissolving the polymer (approximately 20-50 mg) in  $\text{CDCl}_3$  (approximately 1 mL) and charging the resulting solution to a 5 mm NMR tube.

Number-average molecular weight ( $M_n$ ) values and polydispersity index (PDI) values were obtained via gel permeation chromatography (GPC) using a Waters 2695 separation module, a Wyatt miniDAWN TREOS Multi-Angle static Light Scattering (MALS) detector, and a Wyatt Optilab T-rEX differential Refractive Index (dRI) detector. Sample solutions were run through a series of two 30 cm columns with parameters best suited to their expected molecular weights: prepolymer samples utilized columns intended for materials expected to have  $M_n$  values under 30,000 g/mol (Agilent PLgel mixed-E, 3  $\mu\text{m}$  bead size), while copolymers used a setup capable of detecting  $M_n$  values up to 400,000 g/mol (Agilent PLgel mixed-D, 5  $\mu\text{m}$  bead size). The mobile phase was freshly distilled THF, delivered at a flow rate of 1.0 mL/min. Sample concentrations were approximately 5 mg polymer/mL THF, and the injection volume was 100  $\mu\text{L}$ . The detector signals were recorded using ASTRA software (Wyatt Technology Inc.) and the molecular weight values were determined by MALS using a refractive index increment ( $dn/dc$ ) value either reported in literature for known samples (such as polyamides), or calculated from the dRI response assuming a 100% mass recovery of the sample from the columns for unreported materials (PIB-PA copolymers).

Isobutylene polymerizations were carried out under a N<sub>2</sub> atmosphere in a glove box (MBraun Labmaster 130) equipped with thermostatted heptanes cooling bath and a ReactIR 45m reaction analysis system (Mettler-Toledo) to enable real-time attenuated total reflectance Fourier transform infrared (ATR-FTIR) spectroscopic monitoring of monomer conversion. The polymerization was tracked by monitoring the decrease of the area of the absorbance peak centered at 887 cm<sup>-1</sup>, representative of the double bond present in the isobutylene monomer that disappears upon polymerization.

Matrix-assisted laser desorption/ionization time-of-flight mass spectrometry (MALDI-TOF MS) was carried out on a Bruker Microflex MALDI-TOF spectrometer. Polyamide samples were prepared using the solvent-free method<sup>19</sup> wherein approximately 1-2 mg of polyamide was weighed into a mortar, followed by 5-10 mg of 2,5-dihydroxybenzoic acid to serve as matrix (to aim for a 1:5 weight ratio of sample:matrix). The reagents were then combined using a pestle, and placed onto a stainless steel MALDI target plate for analysis.

### **2.2.3 Synthesis and characterization of polyisobutylenes**

#### **2.2.3.1 Synthesis of $\alpha,\omega$ -bis[4-(3-bromopropoxy) phenyl]polyisobutylene**

Difunctional PIB samples with primary bromine terminations were synthesized using living carbocationic polymerization techniques previously reported,<sup>18</sup> utilizing bDCC initiator and TiCl<sub>4</sub> co-initiators in a 40/60 (v/v) hexane/methyl chloride cosolvent system at -70 °C with 3-phenoxypropyl bromide as quencher. A representative procedure was as follows: in an N<sub>2</sub> atmosphere, 138 mL of hexane and 208 mL of methyl chloride were placed into graduated cylinders and chilled in the heptanes bath to -70 °C. They were then added to a 1 L four-neck round bottom flask which was also immersed in the

heptanes bath and equipped with an overhead stirrer, thermocouple, and ReactIR probe. The flask was then charged with 0.16 mL (1.4 mmol) of 2,6-lutidine followed by addition of 7.99 g (27.8 mmol) of bDCC initiator. After the temperature of the reactor contents had stabilized, 112 mL (1.40 mol) of isobutylene was added, and polymerization was initiated by the addition of 0.37 mL  $\text{TiCl}_4$ , followed by an additional 0.30 mL of  $\text{TiCl}_4$  after 10 min (total 6.1 mmol). The mixture was allowed to react until the  $887\text{ cm}^{-1}$  peak had essentially disappeared (approximately 1 h). At that point, 21 mL (0.13 mol) of 3-phenoxypropyl bromide and 14 mL (0.13 mol) of  $\text{TiCl}_4$  were added to the flask in order to quench the reaction, a process expected to reach completion after 2-3 h. The contents were allowed to mix for 18 h before approximately 50 mL (1.23 mol) of chilled methanol was added to the flask in order to terminate the reaction. The flask was removed from the  $\text{N}_2$  atmosphere and allowed to warm to room temperature with evaporation of methyl chloride. The product was then further diluted with n-hexane (for a total volume of approximately 300 mL) and transferred to a separatory funnel where any remaining methyl chloride was removed. The PIB-hexane solution was then precipitated into methanol (approximately 1,400 mL) and allowed to sit overnight. The methanol layer was decanted and the PIB product re-dissolved into n-hexane, then washed three times with methanol followed by three washes with DI water. The solution was dried over  $\text{MgSO}_4$  and then filtered, and the polymer was isolated by stripping the solvent via rotary evaporation followed by further solvent removal under vacuum. The final mass of the polymer was 97 g, giving a yield of 97%.



### **2.2.3.2 Synthesis of $\alpha,\omega$ -bis[4-(3-phthalimidopropoxy)phenyl] polyisobutylene**

Bromine-terminated difunctional PIB (97g; 3,450 g/mol; synthesized as described above) was dissolved into a 2:1 (v/v) mixture of THF (300 mL) and NMP (150 mL) in a 1 L round bottom flask equipped with a magnetic stir bar. Potassium phthalimide (17 g, 92 mmol) was added, and the flask was equipped with a condenser. The flask was lowered into a heating oil bath (100 °C) and set to stir. The contents were reacted at reflux for 5 h, after which the flask was removed from the oil bath and allowed to air cool. The contents were dissolved in n-hexane and transferred to a separatory funnel, where the product layer was isolated. After precipitation into methanol, the product was washed three times each with methanol and DI water before being dried over MgSO<sub>4</sub>. After removal of the MgSO<sub>4</sub> by filtration, the product was dried using rotary evaporation followed by further solvent removal under vacuum. The final mass of the polymer was 93.97 g, resulting in a yield of 97%.

### **2.2.3.3 Synthesis of $\alpha,\omega$ -bis[4-(3-aminopropoxy)phenyl] polyisobutylene**

Phthalimide-terminated difunctional PIB (94 g, synthesized as described above) was dissolved in a 1:1 (v/v) mixture of heptanes and ethanol (300 mL) in a 1 L round bottom flask. An excess of hydrazine monohydrate (14 g) was added to the flask, and the contents set to stir with a magnetic stir bar. The flask was equipped with a condenser, and lowered into a heating oil bath (approximately 105 °C). The contents reached reflux and were allowed to react for 5 h before the flask was removed from heat and allowed to air cool. Hexane was added to the flask and the contents moved to a separatory funnel, where the product layer was isolated before precipitation into methanol. The solution was then washed with methanol and DI water two times each, ridding the product of any

excess hydrazine monohydrate. After drying over  $\text{MgSO}_4$  to remove residual water, the solution was filtered, and the solvent was removed by rotary evaporation and subsequent vacuum evaporation. The final product had a mass of 81.16 g, resulting in a yield of 86%.

#### **2.2.3.4 Characterization of polyisobutylenes**

Molecular weight of the polyisobutylene was determined using GPC-MALS. The  $dn/dc$  value of the sample was calculated from the refractive index detector response, assuming 100% mass recovery from the columns. The sample solution was at a concentration of 5 mg/mL THF. The  $M_n$  and PDI of the bromine-terminated PIB were determined to be 3,450 g/mol and 1.17, respectively.

Structure and end-group functionality of the PIB synthesized as described above was characterized at each of its different end-group stages using  $^1\text{H}$  NMR spectroscopy, the spectra of which are shown in Figure 2.1 (including selected peak assignments and integrations).

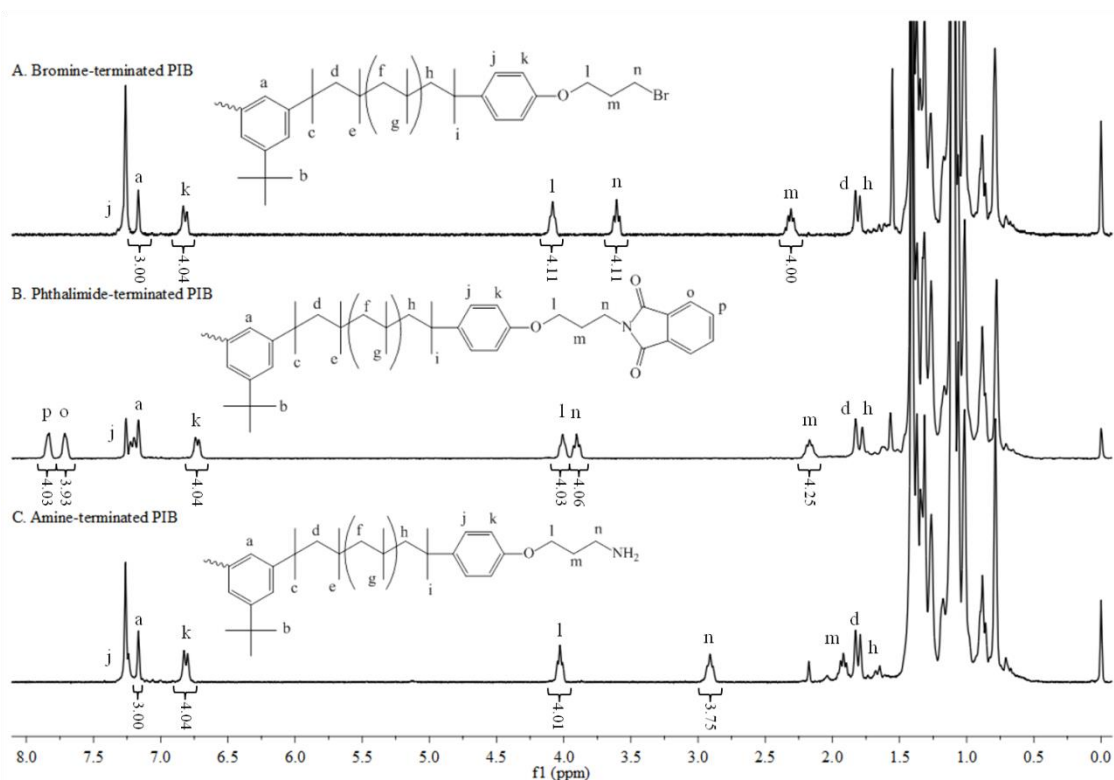


Figure 2.1  $^1\text{H}$ -NMR spectra of (A)  $\alpha,\omega$ -bis[4-(3-bromopropoxy)phenyl]polyisobutylene, (B)  $\alpha,\omega$ -bis[4-(3-phthalimidopropoxy)phenyl]polyisobutylene, and (C)  $\alpha,\omega$ -bis[4-(3-aminopropoxy)phenyl]polyisobutylene.

Effectiveness of the (3-bromopropoxy)benzene quencher is shown in spectrum A of Figure 2.1 by the appearance of peaks j (7.26 ppm) and k (6.81 ppm), representative of the aromatic ring protons present in the quencher. Peaks l (4.08 ppm), n (3.61 ppm), and m (2.31 ppm) are indicative of the methylene protons of the three-carbon tether holding the primary bromine terminus. Integrations of these three peaks all approximate 4.00 when normalized to a 3.00 integration of the peak representative of the protons located on the aromatic initiator moiety, indicating that the sample consists of fully bromine-functionalized telechelic PIB chains. The first step of a Gabriel synthesis was then carried out, replacing the bromine end groups with phthalimide moieties by reaction of the PIB with potassium phthalimide. Spectrum B in Figure 2.1 shows the successful addition of

the phthalimide end groups by the appearance of peaks p (7.83 ppm) and o (7.72 ppm) within the aromatic region. The change in end functionality is also evidenced by the downfield shift of peak n, representing the ultimate methylene unit of the tether, from 3.61 ppm to 3.90 ppm. Again, integrations of peaks corresponding to the phthalimide resonances all approximate 4.00, suggesting full functionalization of the bromine end groups to phthalimide. In the second and final step of the Gabriel synthesis, the phthalimide-terminated PIB was reacted with hydrazine monohydrate to replace the phthalimide end groups with amine terminations. In going from spectrum B of Figure 2.1 to spectrum C, one can note the disappearance of the peaks representing the aromatic protons of the phthalimide group (peaks p and o), and the upfield shift of peak n from 3.90 ppm to 2.92 ppm.

## **2.2.4 Synthesis and characterization of polyamides**

### **2.2.4.1 Synthesis of polyamides**

Four different types of carboxylic acid-terminated polyamides were synthesized in bulk polycondensation reactions: polyamide-6 (PA-6), polyamide-11 (PA-11), polyamide-12 (PA-12), and polyamide-6,6 (PA-6,6). The appropriate monomers and amounts needed of each to form the desired polymer are reported in Table 2.1. It should be noted that the synthesis of PA-6 also required the addition of a small amount of DI water to catalyze the ring-opening reaction.

Table 2.1

## Polyamide formulations and yields

PA Type	Monomer used (g)					Pre-Soxhlet		Post-Soxhlet	
	AA	$\epsilon$ -CAP, 6-ACA	11- AUA	12- ADA	HMD	Mass (g)	Yield* (%)	Mass (g)	Yield (%)
PA-6	2.00	20.32, 1.80	---	---	---	22.95	111.30	4.93	23.92
PA-11	1.77	---	11.26	---	---	11.62	96.63	9.67	80.48
PA-12	1.75	---	---	11.12	---	11.78	98.69	8.81	73.84
PA-6,6	10.50	---	---	---	6.62	14.75	91.67	11.90	73.94

Amounts of monomers used in synthesis of all polyamide variations, as well as masses of products and yields of reactions both pre- and post-Soxhlet extraction. Pre-Soxhlet yields may appear as greater than 100% due to water trapped inside the product, which is eventually washed out during the Soxhlet extraction process.

A representative synthesis (for PA-12) was carried out as follows: 12-ADA (11.12 g) and AA (1.75 g) were added to a one-neck round bottom flask along with a magnetic stir bar. The flask was also equipped with a Claisen adapter, which was closed with rubber septa and supplied with N<sub>2</sub> inlet and outlet lines. The flask was lowered into a preheated oil bath (210 °C), and stirring and a N<sub>2</sub> purge were applied. The contents were allowed to react for 4 h, after which the flask was removed from heat and allowed to air cool. The resultant polymer plug was broken out of the flask and crushed into a powder using a mortar and pestle. The powder was then placed into a cellulose thimble and into a Soxhlet apparatus, where it underwent Soxhlet extraction by methanol for 24 h followed by drying in a vacuum oven. The polymer weighed 11.78 g before Soxhlet extraction, for a crude yield of approximately 99%--though this calculated yield may have included water trapped in the product that would eventually be washed out during extraction. Post-Soxhlet extraction the polymer weighed in at 8.81 g, for a purified yield of 74%.

#### 2.2.4.2 Trifluoroacetylation of polyamides for GPC characterization

Approximately 0.05 g of polyamide was weighed into a scintillation vial, with mass being recorded to the nearest milligram. DCM (2.5 mL) and TFAA (1 mL) were then added, and the vial was recapped and placed on a wrist shaker. After 19 h of reaction, solvent and any excess anhydride were removed via rotary evaporation for 30 min at 30 °C.<sup>20</sup> The mass of the post-trifluoroacetylation polymer was taken, and THF added in an appropriate amount to target a solution with a concentration appropriate for GPC (5 mg polymer/mL THF). The resultant molecular weights are reported in Table 2.2, and were calculated using a literature-reported  $dn/dc$  value (0.1060 mL/gm in THF at 23 °C).<sup>21</sup>

Table 2.2

Polyamide molecular weights as determined by GPC, titration, and MALDI-TOF MS

Polyamide Type	$M_n$ (g/mol)		
	GPC	Titration	MALDI
PA-6	1640	1209	1304
PA-11	1440	1344	1358
PA-12	2450	1585	1604
PA-6,6	1760	1575	916

Molecular weight values as determined by GPC reported above are those of the polymer after undergoing trifluoroacetylation.

Because the titration and MALDI-TOF MS values are in better agreement and represent the unmodified polymer, these values were the ones used in calculating the mass necessary for PIB-PA copolymerization.

#### 2.2.4.3 Titration of polyamides for molecular weight determination

Approximately 0.5 g of carboxylic acid-terminated polyamide was weighed into an Erlenmeyer flask, with mass being recorded to the nearest milligram. Benzyl alcohol was added (25 mL), as well as several drops of a solution of cresol red (1 wt% solution in

2-propanol) to act as indicator, along with a magnetic stir bar. The flask was placed in an oil bath heated to 120 °C and the contents set to stir. Once the PA was fully dissolved, a standardized solution (approximately 0.1 *M*) of KOH in 2-propanol was added dropwise to the heated flask using a burette. The previously yellow solution was titrated to a violet end point, and the volume of titrant required was recorded and used to calculate the molecular weight of the PA material, assuming linear, difunctional molecules. Resultant molecular weights can be seen in Table 2.2.

#### **2.2.4.4 MALDI-TOF MS of polyamides**

Polyamide samples were prepared for MALDI-TOF MS analysis for molecular weight determination and structure confirmation via the solvent-free method. A representative MALDI-TOF spectrum for PA-11 showing intensity vs. mass/charge ratio can be seen in Figure 2.2. The main plot shows intensity versus mass/charge ratio, and displays three distributions—the most intense one represents the protonated PA sample, and the two minor distributions come from ionized potassium and sodium adducts. The inset plot in Figure 2.2 shows the mass/charge ratio versus degree of polymerization for the protonated sample distribution. The slope of the resulting line represents the mass of the observed repeat unit, and the intercept accounts for the mass of the end groups of the polymer. In the case of PA-11, we would expect the repeat unit based on 11-AUA (accounting for water loss) to weigh approximately 183.289 g/mol, and the end group, comprised of one unit of AA, to weigh approximately 146.142 g/mol. Indeed, the resulting fit line seen in Figure 2.2 agrees with these expectations: a slope of 183.7 g/mol and intercept of 146.96 g/mol supports the structure of the PA-11 as being repeating units

of 11-AUA with carboxylic acid end groups. Molecular weights were also calculated from the MALDI-TOF spectrum, and can be found in Table 2.2.

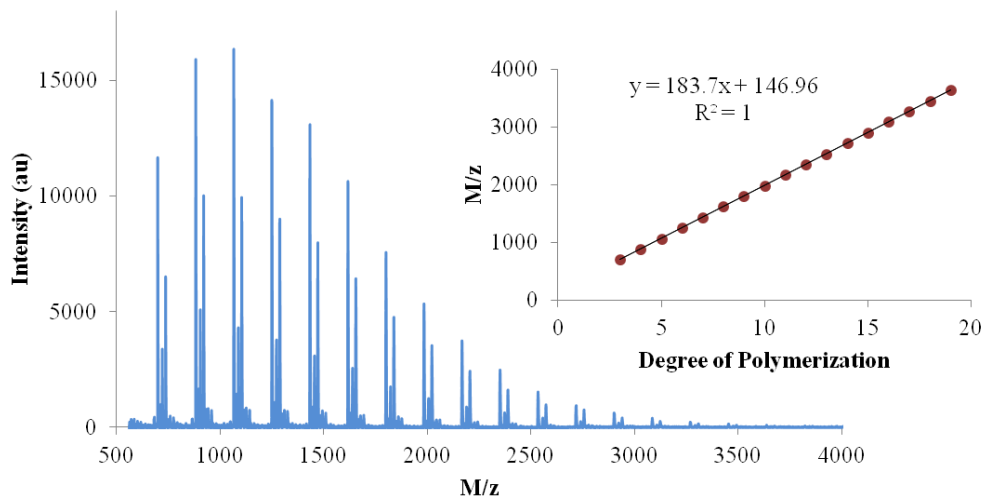


Figure 2.2 MALDI-TOF MS spectrum for PA-11.

The main plot shows intensity versus mass/charge ratio, while the inset plot shows mass/charge ratio versus degree of polymerization.

Similar plots for the other three varieties of PA examined can be found in Appendix A: PA-12 is shown in Figure A.1, PA-6 is shown in Figure A.2, and PA-6,6 is shown in Figure A.3. A table showing the agreement between the expected and experimental values for molecular weights of the repeat units and end groups of all PA varieties can also be found in Appendix A (Table A.1).

### 2.2.5 Synthesis of polyisobutylene-*block*-polyamide copolymers

After syntheses of the polyisobutylene and polyamide prepolymers were carried out as described above, the two materials were combined to create a variety of PIB-PA copolymers. Though amounts and types of the prepolymers used differed, the general synthesis was consistent among PIB-PA batches. A representative synthesis (of 3:1 PIB-PA 11) went as follows:



Difunctional amine-terminated PIB (15.423 g) with an approximate molecular weight of 4,500 g/mol was loaded into a three-neck round bottom flask. The flask was then charged with difunctional carboxylic acid-terminated PA 11 (1,425 g/mol) in an amount necessary to maintain a 1:1 molar ratio of the components, meaning a 3:1 weight ratio of PIB:PA (4.877 g of PA 11). A glass stir rod with Teflon stir piece was placed in the center neck of the round bottom, equipped with a glass vacuum stirrer adapter. Nitrogen gas inlet and outlet lines were provided using the other two necks of the flask, and a nitrogen gas purge was applied to the flask contents as an oil bath was preheated to 200 °C. The glass stir rod was attached to a mechanical stirrer, and stir speed (approximately 60 rpm) was controlled using a dual motor controller. The flask was lowered into the oil bath, stirring was initiated, and the contents allowed to react for 16 h.

#### **2.2.5.1 Design of Experiments (DOE)**

In the synthesis described above, the reaction temperature employed was 200 °C, and the time of reaction was 16 h. These parameters were not arbitrary, but instead chosen based on a design of experiments employed to find the optimal conditions for the PIB-PA copolymerization.

Previously, PIB-PA polymerizations using magnetic stirring were run for 5 h at 215 °C. However, the viscosity of the forming copolymer seemed to eventually become too high for the magnetic stirring to be effective, as the stir bar was unable to freely rotate in the increasingly viscous product. This inability of the stir bar to efficiently move was noticed around the 1-2 h mark of polymerization, and it was therefore thought that the additional polymerization time being applied was unsuccessful in further reaction of the prepolymers. Additionally, when mechanical stirring was employed and the material was

more efficiently mixed through the duration of the reaction, it was unknown at what point the reaction could be stopped with confidence that the material had reacted as closely to completion as possible. Therefore, a Design of Experiments (DOE) was created in order to determine at what conditions the PIB-PA reaction should be run in order to maximize molecular weight of the product (indicative of a better mechanical performance) while not subjecting the reaction to excess time or temperature.

#### **2.2.5.1.1 Experimental**

A full factorial experiment was designed, with input variables of temperature (200 °C and 220 °C) and time (1 h, 4 h, 7 h, 10 h), and an output variable of molecular weight (measurable by GPC). Three runs were completed at each temperature and an aliquot taken at each time point given above, to gather a total of 24 data points for the DOE analysis.

Amine-terminated PIB (approximately 3,080 g/mol) and carboxylic acid-terminated PA-11 (approximately 1,690 g/mol) were combined in a mass ratio appropriate to target a 3:1 molar ratio of PIB:PA. The prepolymers were loaded into a three-neck round bottom flask: one neck was equipped with nitrogen inlet/outlet lines, the center neck with a mechanical stir rod, and the third neck sealed with a rubber septum that was removed in order to collect aliquots. Controlled variables included the speed of mechanical stirring (via use of a dual motor control set to rotate the mechanical stir rod at 60 rpm) and the molar ratio of the samples. Moisture content existed as an uncontrolled variable, though it was attempted to be made consistent by the use of nitrogen purge during the reactions. The samples collected for each aliquot underwent trifluoroacetylation in order to determine the molecular weight of the material via GPC.

As the prepolymers utilized in this experiment were not proven to be fully difunctional, the molecular weights of the copolymers measured are to be used in a comparative manner against the other trials in the experiment, and not viewed as the maximum molecular weights achievable for PIB-PA materials. Observed molecular weights can be seen in Table 2.3.

Table 2.3

Design of Experiments molecular weight results

Run Number	Temp (°C)	M <sub>n</sub> (g/mol) at Time (h):			
		1	4	7	10
1	220	5891	6510	9302	8319
2	200	4049	5302	6389	7604
3	220	4566	7417	8364	11210
4	220	4506	7021	7352	7258
5	200	4633	5824	7451	12780
6	200	5891	6510	9302	8319

Molecular weights collected via GPC of samples having undergone trifluoroacetylation are given for each data point (every time point of every run) gathered during the Design of Experiments.

### 2.2.5.1.2 Results

One-way analysis of variance (ANOVA) tests were run on each of the input variables to determine if either factor made any significant contribution to the changes observed in molecular weight during the PIB-PA copolymerization. The null hypothesis for each analysis stated that there was no difference among the two different populations; for example, for the input variable of temperature, the null hypothesis predicts that the average molecular weight for samples created at 200 °C will not significantly differ from the molecular weights seen in samples created at 220 °C. The  $\alpha$  value was defined as 0.05. A calculated p-value of less than 0.05 meant that the null hypothesis was rejected,

whereas a p-value greater than that of  $\alpha$  meant that there is not sufficient evidence to reject the null hypothesis. The p-values for these experiments as calculated by statistical package Minitab can be seen in Table 2.4.

Table 2.4

ANOVA Calculated p-values

Input variable	p-Value
Temperature	0.730
Time	0.000

The p-values for each input variable tested during the Design of Experiments are given above. These values were compared to the chosen  $\alpha$  value of 0.05.

The p-value calculated for the input variable of temperature was 0.730, a value greater than the defined  $\alpha$  of 0.05. This means there is not sufficient evidence to reject the null hypothesis: it cannot be said that the difference in temperatures tested has a significant effect on the molecular weights of the formed copolymers. The p-value found for the input variable of time, however, was virtually zero: as this is much lower than the chosen  $\alpha$  of 0.05, the null hypothesis can be rejected. This means that changing the reaction time of the copolymerization has a statistically significant effect on the molecular weight of the final product. These results can be visualized in interval plots, as seen in Figure 2.3.

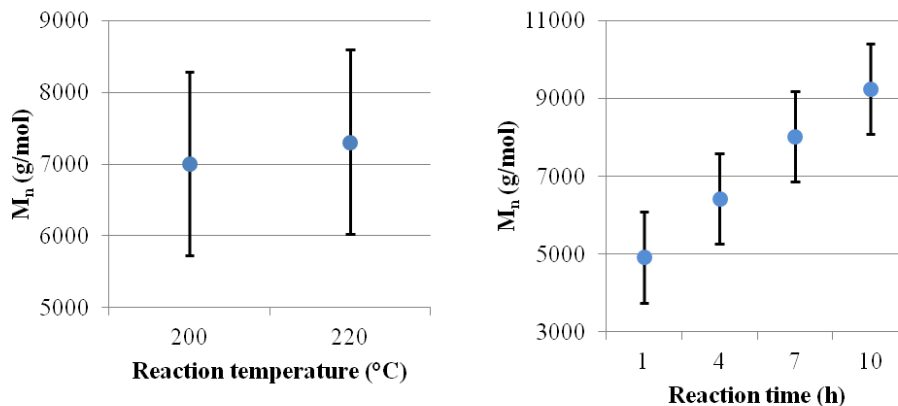


Figure 2.3 Design of Experiments molecular weight interval plots.

The chart on the left shows the 95% confidence intervals for molecular weight data when the studied input variable is reaction temperature, while the chart on the right displays the intervals for the input variable of reaction time.

The left chart of Figure 2.3 shows the 95% confidence interval for the molecular weight data when categorized by reaction temperature. As one can see, the average molecular weights are very similar, and the intervals cover virtually the same range. In the chart on the right, however, one can see that the confidence intervals for different reaction times show a larger spread. There is no overlap whatsoever between the full ranges for the 1 h and 10 h time points. This supports the statistical data in showing that variation of reaction time indeed has an effect on molecular weight of the PIB-PA copolymer: more specifically, an increase in reaction time correlates to an increase in the molecular weight.

These results allow for the determination of reaction parameters in future PIB-PA copolymerizations. Since reaction temperature did not have a marked effect on final molecular weight, either temperature could serve as an appropriate choice. The use of a lower temperature offers many advantages in any chemical reaction: increased safety, a lower chance of side reactions, and lower incurred expenses are just a few examples.

Therefore, 200 °C was chosen as the reaction temperature to be used in any copolymerizations going forward. (The exception to this is the copolymerization of PIB and PA-6,6: the polyamide's melting point was found by differential scanning calorimetry to be 242 °C, so a higher reaction temperature of 270 °C was chosen to fully melt both reactants.) Reaction time was shown to have significance in the molecular weight of the product; however, an upward trend in molecular weight was witnessed, and no plateau reached during experimentation. This means that molecular weight could potentially be continuing to significantly increase beyond the 10 h of reaction completed in this study. Therefore, a PIB-PA copolymerization longer than 10 h was carried out in order to identify at what time significant molecular weight increase ceases to occur in the final product.

#### **2.2.5.2 Extended time PIB-PA copolymerization**

As seen in the interval plot in Figure 2.3 studying time as the input variable, molecular weight of the PIB-PA copolymer appeared to be increasing in a linear fashion between 1 h and 10 h of reaction time. A plateau was expected to appear at the point when all prepolymer had reacted to form copolymer; however, such a plateau did not appear in the 10 h time frame. Therefore, it was thought that 10 h was not a long enough reaction time to reach this maximum conversion, and an extended PIB-PA copolymerization was carried out in order to determine that optimal reaction time.

Difunctional amine-terminated PIB (3,450 g/mol, 5.040 g) and difunctional carboxylic acid-terminated PA-11 (1,340 g/mol, 1.969 g) were loaded into a three-neck round bottom flask. A N<sub>2</sub> purge was applied, and the flask lowered into an oil bath heated to 200 °C. One neck of the flask housed a glass rod with a Teflon stir piece, responsible

for mechanical stirring of the reactants at a consistent rate (approximately 55 rpm) via use of a dual motor controller. Aliquots were taken over a 12 h time period. Molecular weights of the samples were determined via GPC after trifluoroacetylation of the copolymers. However, once more, a steadily increasing molecular weight trend was seen, with no plateau appearing before the end of the experiment. Therefore, an even longer reaction of 48 h was carried out using the same starting materials and procedure as given above. Post-trifluoroacetylation molecular weights of the aliquots as determined via GPC from both experiments can be seen in Table 2.5 and a graphical representation of the resulting molecular weight trend can be seen in Figure 2.4.

Table 2.5

Molecular weights of PIB-PA samples from extended copolymerizations

Time (h)	M <sub>n</sub> (g/mol)
5	22410
7	23880
8	27620
9	27290
10	32320
12	37630
24	34060
40	39830
44	48100
48	39510

Reported molecular weights are those of the polymers after having undergone trifluoroacetylation. The aliquots from 5 h to 12 h were taken during the 12 h extended copolymerization reaction, and the aliquots from 24 h to 48 h were taken during the 48 h reaction..

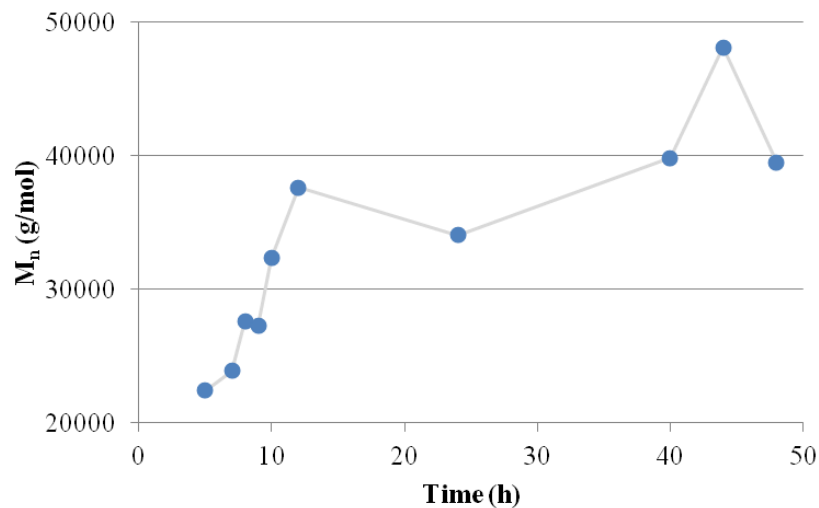


Figure 2.4 Molecular weights of PIB-PA samples from extended copolymerizations

Displayed  $M_n$  values are those of the polymer after trifluoroacetylation. The first 6 data points are from the 12 h extended copolymerization, while the subsequent 4 data points are from the 48 h copolymerization.

As seen in Figure 2.4, molecular weight of the copolymer appears to increase in a semi-linear fashion through 12 h of polymerization. Molecular weights of aliquots taken in the 24 h to 48 h time frame, however, seem to vary within a limited range. It is believed that this variance in molecular weight is due to potentially inconsistent stirring as the material becomes more viscous at longer reaction times. An overall trend in the behavior of the molecular weight of the PIB-PA can be seen by viewing the light scattering traces collected during GPC analysis of the material. The inset plot of Figure 2.5 highlights the peaks of the light scattering traces collected during GPC of the samples taken during both the 12 h and the 48 h reactions.



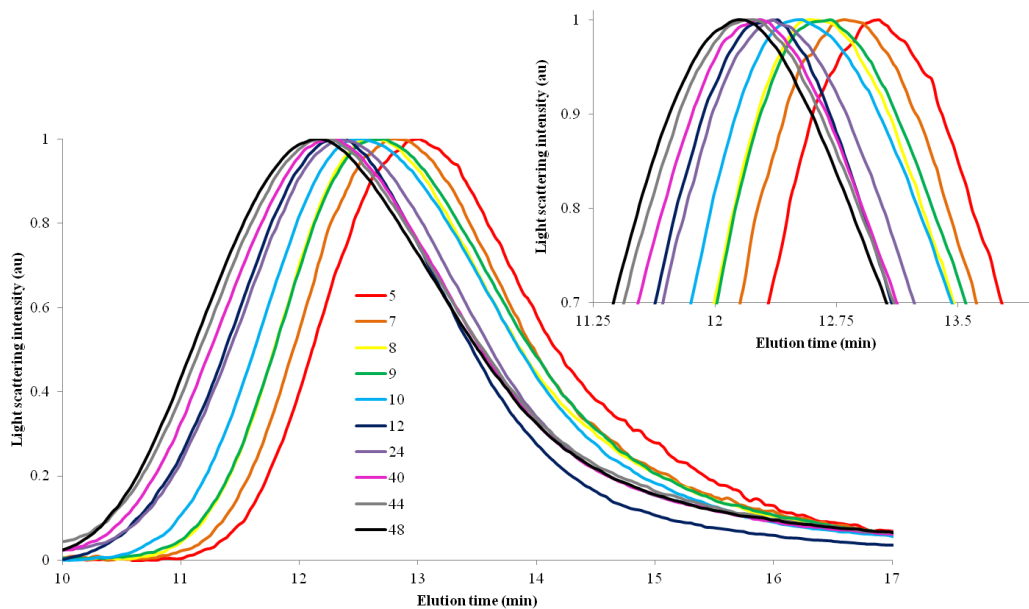


Figure 2.5 GPC light scattering traces of 48 h copolymerization aliquots.

The aliquots taken at 5 h through 12 h were collected during the 12 h copolymerization, and the 24 h through 48 h aliquots were collected during the subsequent 48 h copolymerization. The main plot shows the full traces, while the inset plot shows a focused view of the peaks of the traces.

The new time points collected during the 48 h trial do display shorter elution times, indicating a higher molecular weight was reached. However, it can be seen that the distance between peaks grows shorter and shorter as reaction time increases, suggesting that any increase seen in molecular weight at the higher time points is not as significant as the increases seen in the first 12 h of reaction. Therefore, a reaction time of 16 h was chosen for all subsequent PIB-PA copolymerizations.

### 2.2.5.3 Ladder study

Previously, Kucera completed a “ladder” study in which molecular weight of PIB-PA copolymer product was determined as a function of the stoichiometric ratio of PIB amine end groups and PA carboxylic acid end groups in the prepolymer feed.<sup>15</sup> The results of this study showed, as one might expect of fully difunctional precursors, the

exact 1:1 molar ratio product (50% PIB, 50% PA) resulted in the highest molecular weight. However, there was no distinguishable trend to be found in the ladder study results: while one might expect to see a curve showing molecular weights increasing as molar ratios approach a 1:1 value from either side, the resultant plot (Figure 1.3 as seen in Chapter I) instead shows a somewhat random collection of data points where the highest molecular weight sample happens to be at the 50% PIB mark. In fact, the lowest molecular weight found during the study was the adjacent data point, at 51% PIB. Therefore, it was desired to complete a more exacting ladder study. Such a study could show whether trends were visible on a smaller interval scale, or otherwise show that GPC results for PIB-PA copolymers that have undergone trifluoroacetylation are not appropriate for detecting changes in molecular weights of materials with such minute formulation adjustments.

#### **2.2.5.3.1 Experimental**

Difunctional amine-terminated PIB (3,450 g/mol) was combined with difunctional carboxylic acid-terminated PA-11 (1,440 g/mol) in an amount appropriate to target the desired molar ratio of PIB:PA between 48% and 52% PIB (a full list of ratios achieved by the nine samples synthesized can be seen in Table 2.6). The precursors were loaded into a test tube which was equipped with a glass stir rod and Teflon stir piece. The tube was sealed with a rubber septum containing an opening allowing the addition of the glass stir rod while maintaining a closed system. The stir rod was then attached to a mechanical stirrer, which mixed the contents at approximately 60 rpm as the test tube was suspended in an oil bath heated to 200 °C. After 16 h of reaction, heat and stirring were stopped, and the material allowed to cool. The copolymer plug was then broken out

of the test tube and subjected to trifluoroacetylation as previously described in order to use GPC for molecular weight determination. The molecular weights found for each sample are reported in Table 2.6, and the results can be graphically observed in Figure 2.6.

### 2.2.5.3.2 Results

Table 2.6

Mechanical stirring ladder study molar ratios and resultant molecular weights

Sample	Molar % PIB	M <sub>n</sub> (g/mol)	dn/dc (mL/g)
1	48.014	81,410	0.0700
2	48.514	88,640	0.0692
3	49.059	23,480	0.0582
4	49.441	89,390	0.0643
5	49.820	249,600	0.0604
6	50.169	35,600	0.0720
7	50.415	200,960	0.0551
8	51.026	100,700	0.0642
9	52.053	228,300	0.0633

All reported molecular weights are those of the PIB-PA copolymer after having undergone trifluoroacetylation.

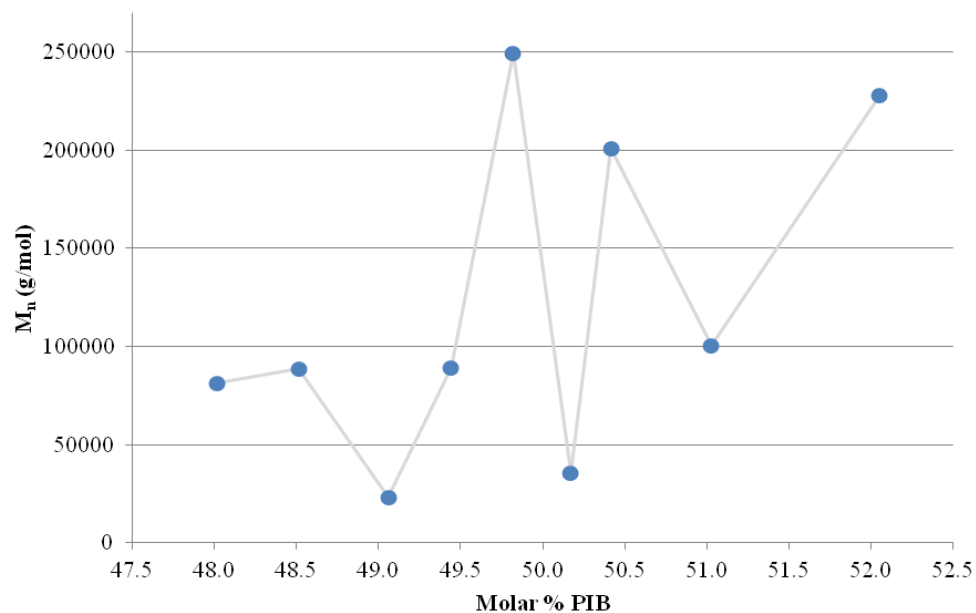


Figure 2.6 Mechanical stirring ladder study molecular weights.

Shown molecular weights are those of the polymer after having undergone trifluoroacetylation.

As in the previous ladder study, no clear trend is visible in Figure 2.6, and the variance seen among the molecular weights is even higher. Sample 5, which is comprised of just under 50% PIB, displays the highest molecular weight (249,600 g/mol), while Sample 6, a sample with just over 50% PIB, has one of the lowest (35,600 g/mol). It was therefore decided that in this instance, GPC is not an appropriate method to differentiate molecular weight changes between materials with such miniscule differences in formulation. There are multiple potential reasons for why these molecular weight values are in such disagreement. First, the nature of the mechanically stirred test tube reaction allows for potentially inconsistent stirring—some material might be completely stirred for the duration of the 16 h, resulting in a higher molecular weight, while some material might avoid the stir paddle for a portion of time, meaning its molecular weight does not continue to increase. Because such small sample sizes are used for the

trifluoroacetylation process, the resultant molecular weight is not always an accurate representation of the batch as a whole. Additionally, and more likely the primary cause of inconsistency, the small scale of the trifluoroacetylation process means that any amount of residual solvent or impurity in the system could skew the molecular weights calculated from light scattering data following the GPC testing. As seen in Table 2.6, the  $dn/dc$  values calculated for the samples taken during the ladder study range from 0.0551 to 0.0720 mL/g. We would expect these values to be more consistent considering the miniscule changes made between samples (slight variation in weight ratio of components). This tells us that the samples did not necessarily behave uniformly during trifluoroacetylation—one sample might have more residual solvent in it than another, or perhaps one sample did not experience full replacement of the amide hydrogens with trifluoroacetate groups, causing it to not be fully soluble in THF for GPC characterization.

However, some of the molecular weights (especially those data points over 200,000 g/mol) seen during the ladder study are much higher than previously achieved by PIB-PA copolymer samples, inspiring hope that better mechanical properties will also be present in material with a higher weight ratio of soft block.

## CHAPTER III – MECHANICAL AND THERMAL PROPERTIES OF POLYISOBUTYLENE-*BLOCK*-POLYAMIDE THERMOPLASTIC ELASTOMERS

The previous chapter focused on improving synthesis of starting materials and the PIB-PA copolymerization process with the end goal of optimization of the PIB-PA TPE molecular weight. However, molecular weight serves only as a predictor of material behavior: the true indicator of a successful TPE lies in its actual mechanical properties. The properties of PIB-PAs synthesized using mechanical stirring and formulated with an increase in PIB content were assessed using various thermal and mechanical testing techniques. The results were then compared to those of earlier PIB-PA formulations, as well as commercial Pebax<sup>®</sup> materials.

### **3.1 Experimental**

#### **3.1.1 Materials**

New PIB-PA materials were synthesized as described in Chapter II (utilizing mechanical stirring and PIB:PA weight ratios of 3:1), and the resultant data was compared to that of the samples previously synthesized by Kucera (magnetically stirred batches with targeted PIB:PA weight ratios of 1:1 and 2:1).<sup>15</sup> Various types of Pebax<sup>®</sup> (MP 1878, RNEW 35R53, RNEW 40R53, and RNEW 55R53) were donated by Arkema.

#### **3.1.2 Instrumentation**

Thermogravimetric analysis (TGA) was completed using a TA Instruments Q500 Thermogravimetric Analyzer. Approximately 10-20 mg of polymer was added to a titanium pan and loaded into the furnace, which was continuously purged with N<sub>2</sub> gas at a flow rate of 10 mL/min. The mass of the sample was then recorded as the material was heated from ambient temperature to 600 °C at a rate of 10 °C/min. The degradation

temperature ( $T_d$ ) was determined from the resultant thermogram. Two different temperatures were noted in the following analysis:  $T_{di}$ , the temperature at which the material experiences 5% weight loss from its initial value, and  $T_{dm}$ , the temperature at which the change in mass loss reaches a maximum value (with respect to temperature).  $T_{di}$  was used as a limit in all subsequent work to ensure that the materials did not undergo degradation during any other form of testing or during processing of the material to prepare samples for mechanical testing.

Differential scanning calorimetry (DSC) analysis was completed using a TA Instruments Q100 Differential Scanning Calorimeter. Approximately 5-8 mg of polymer was loaded into a hermetic aluminum crucible, which was then sealed shut using a die press. The pan was then loaded into the cell of the calorimeter, adjacent to an empty reference pan, and the atmosphere of the cell was defined by a 50 mL/min  $N_2$  gas flow. The chosen heating profile started with a temperature ramp at 10 °C/min from ambient temperature to 280 °C to anneal, or erase, the thermal history of the material. The pans were then cooled to -80 °C at a rate of 5 °C/min, held isothermally for 3 min, and then heated again to 280 °C at a rate of 10 °C/min. (One material, PA-6, was only heated to 265 °C on both heating cycles in order to remain safely below the degradation temperature to avoid potential damage of the DSC cell.) The resultant thermograms showing heat flow versus temperature were then examined to detect thermal transitions in the material, such as the glass transition temperature ( $T_g$ ), melting temperature ( $T_m$ ), or crystallization temperature ( $T_c$ ).

Dynamic mechanical analysis (DMA) was performed using a TA Instruments Q800 Dynamic Mechanical Analyzer equipped with a film tension clamp. Three different

DMA tests were completed: a temperature ramp, a room temperature frequency sweep, and a frequency sweep-temperature step experiment. The temperature ramp consisted of equilibrating the sample at -80 °C, holding it isothermally for 5 min, and then ramping to 100 °C at a rate of 5 °C/min at a constant frequency of 1 Hz. During the room temperature frequency sweep, which subjected a sample to one frequency sweep at a single temperature, the sample was equilibrated to 25 °C and held isothermally for 5 min. A frequency sweep from 1 to 200 Hz was then executed isothermally at 25 °C, with data points being collected at 24 different frequencies. The frequency sweep-temperature step experiment subjected a single sample to frequency sweeps at multiple temperatures. The experiment began by equilibrating the sample at -20 °C and holding isothermally for 5 min. A frequency sweep from 1 to 200 Hz was then executed, with data being collected at 24 different frequencies within that range. The temperature was then increased by 20 °C, the sample was held isothermally for 5 min, and then another frequency sweep was implemented. This process was repeated in 20 °C increments, with the final temperature chosen as 80 °C. Material responses recorded throughout each frequency sweep included stiffness, storage modulus, and loss modulus.

Samples for all DMA tests were prepared by loading pelletized polymer into silicone molds to create bars with dimensions of approximately 1.5 mm x 5 mm x 60 mm, and heating the system to a temperature roughly 10 °C higher than the melting point of the material (as found using DSC as stated above) in a Carver melt press. Upon melting of the material, the sample was pressed at approximately 700 psi (the limit of the silicone mold) for about 5 min. Heating was then discontinued, and the plates/mold assembly was



allowed to cool below the melting point of the material. The pressure was then released, and the bars were removed from the flexible molds.

Tensile testing was carried out on an MTS Insight electromechanical testing system (EMTS) equipped with a 500 N load cell. Samples were prepared in the same fashion as described above for DMA bar creation, but using a mold crafted to prepare dumbbell bars following the Type IV specimen dimension guidelines set forth by ASTM D 638.<sup>22</sup> Samples were loaded into a thin film clamp and pulled at a rate of 5 mm/min until break. Tension set testing was also performed according to ASTM 412.<sup>23</sup> Bench marks were made on the reduced section of the specimen, and the distance between them measured. The sample was then loaded into the MTS Insight EMTS and subjected to an extension of 25 mm over 15 s (a rate of 100 mm/min), after which it was held under tension for 10 min. The sample was then released and allowed to recover for an additional 10 min before the distance between benchmarks was re-measured. The percent elongation from the initial measurement was then recorded.

### **3.2 Results**

The procedure for synthesis of PIB-PA copolymers was discussed in Chapter II. Changes made from previous copolymerizations by Kucera<sup>14</sup> in an attempt to increase the performance of the PIB-PA focused on the implementation of mechanical stirring, and increasing the PIB content (length of the PIB segments) of the copolymer. This chapter reports thermal and mechanical testing that was carried out on the new PIB-PA materials in order to compare their properties to the previously synthesized, magnetically stirred PIB-PA formulations, as well as the commercially standard Pebax<sup>®</sup> materials.

### 3.2.1 Thermogravimetric Analysis (TGA)

Thermogravimetric analysis was carried out to determine the decomposition temperature and behavior of the various TPEs being investigated. Figure 3.1 shows TGA thermograms for a PIB-PA 11 copolymer (targeted 3:1 weight ratio of PIB:PA, synthesized as described in Chapter II) and its constituent PIB (4,500 g/mol) and PA-11 (1,425 g/mol) prepolymers. The greatest rate of mass loss ( $T_{dm}$ ) occurs at a higher temperature for the PA (464.15 °C) as opposed to the PIB and PIB-PA (424.76 °C and 428.57 °C, respectively). This suggests that the PA hard segment contributes to the higher  $T_{dm}$  seen in the PIB-PA copolymer.

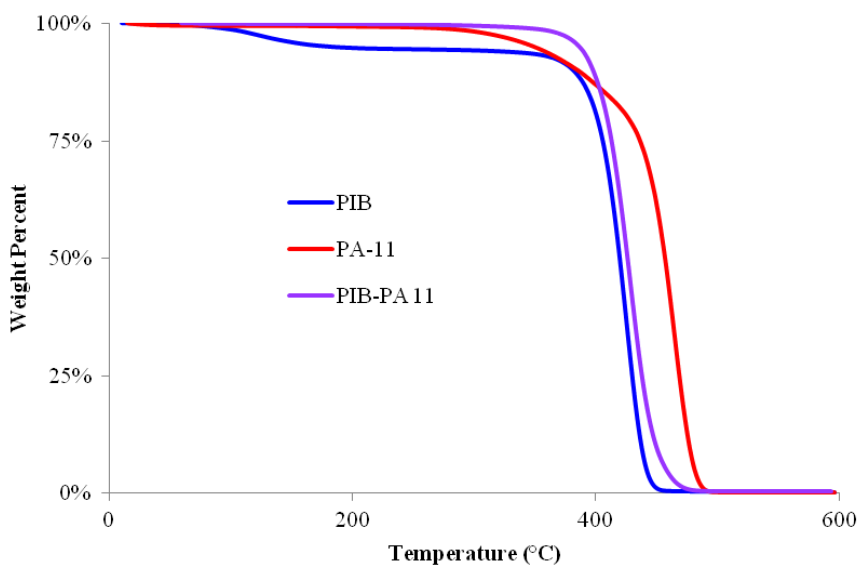


Figure 3.1 TGA thermogram of starting materials (PIB and PA-11) and resulting copolymer.

PIB-PA 11 sample has a targeted PIB:PA weight ratio of 3:1, utilizing 4,500 g/mol PIB and 1,425 g/mol PA. Initial drop in PIB weight percent is due to degradation of residual hexane present in the material.

This idea is further supported by Figure 3.2, which compares the TGA traces of PIB-PA 11 formulations representing various weight ratios of PIB:PA (1:1 and 2:1 PIB:PA samples previously synthesized by Kucera; 3:1 PIB:PA sample synthesized as

described in Chapter II). The temperature at which significant mass loss is occurring the fastest is highest for the 1:1 sample at 457.62 °C, followed by the 2:1 PIB-PA at 449.72 °C, and finally the 3:1 PIB-PA sample at 428.57 °C. This trend shows that as weight percent of the PA decreases in the copolymer formulations, so does the  $T_{dm}$ .

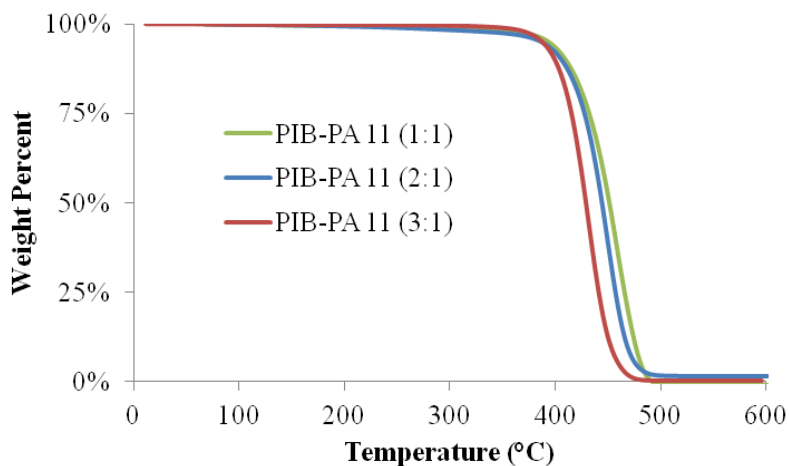


Figure 3.2 TGA thermogram comparison of PIB-PA 11 samples with varying weight ratios.

All samples represented are those utilizing PA of approximately 1,000 g/mol (for 1:1 and 2:1 samples, PA  $M_n$  = 1,020 g/mol; for 3:1 sample, PA  $M_n$  = 1,300 g/mol) with the appropriate molecular weight PIB to achieve the desired weight ratio. Samples targeting PIB:PA weight ratios of 1:1 and 2:1 were previously synthesized by Kucera, while the 3:1 sample was synthesized as described in Chapter II.

TGA of PIB-PAs synthesized from the four different polyamide types showed relatively uniform behavior, shown in Figure 3.3, with all four PIB-PAs displaying essentially the same  $T_{dm}$  value. As reported in Table 3.1, the only outlier was the  $T_{di}$  value of PIB-PA 6, which is approximately 20 °C lower than those of the other PIB-PA varieties.

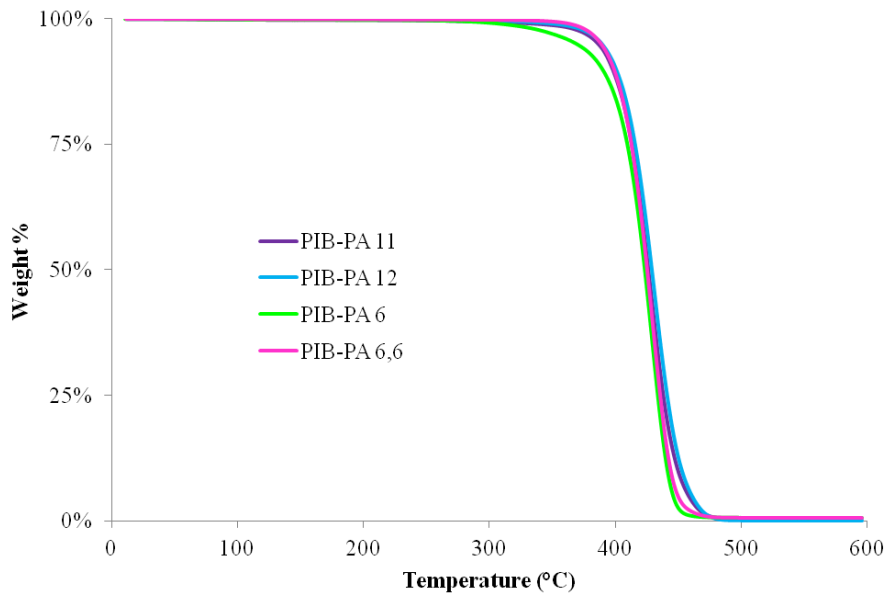


Figure 3.3 TGA thermogram comparison of 3:1 PIB-PA samples.

All PIB-PA samples shown employed a 3:1 weight ratio of PIB:PA using PIB with a molecular weight of approximately 4,500 g/mol and PAs with molecular weights of approximately 1,500 g/mol.

Table 3.1

TGA degradation temperatures for PIB-PA and Pebax<sup>®</sup> TPEs

Material	T <sub>di</sub> (°C)	T <sub>dm</sub> (°C)
PIB-PA 11	386.47	428.57
PIB-PA 12	389.40	430.98
PIB-PA 6	369.58	428.83
PIB-PA 6,6	388.73	429.52
PEBAX 1878	355.15	418.83
PEBAX 35R53	373.77	425.36
PEBAX 40R53	378.48	432.83
PEBAX 55R53	388.20	459.39

All PIB-PA samples represented are those with a targeted 3:1 weight ratio of PIB:PA. T<sub>di</sub> represents the temperature at which the copolymer has experienced 5% mass loss from its initial value, while T<sub>dm</sub> is the temperature at which the material is experiencing its highest rate of mass loss.

A TGA comparison PIB-PA to the Pebax<sup>®</sup> materials shows similar behavior for the two types of TPEs. A plot comparing the TGA thermograms of the four grades of

Pebax<sup>®</sup> to PIB-PA 12 can be seen in Figure 3.4, and accompanying degradation temperatures are recorded in Table 3.1. Only PEBAX 55 displayed a  $T_{di}$  (388.20 °C) that was as high as the  $T_{di}$  values reached by the majority of PIB-PA samples. All other Pebax<sup>®</sup> samples displayed lower  $T_{di}$  temperatures than PIB-PA 11, PIB-PA 12, and PIB-PA 6,6; in fact, PEBAX 1878 was the worst-performing of all TPEs investigated in this regard, with a  $T_{di}$  of only 355.15 °C. The Pebax<sup>®</sup> and PIB-PA materials were more evenly matched in terms of  $T_{dm}$ , however. The PIB-PA materials consistently displayed  $T_{dm}$  values around 429 °C regardless of the PA hard block employed, a value consistent with those displayed by PEBAX 35 and PEBAX 40. The  $T_{dm}$  value shown by PEBAX 55 stood out above its counterparts at 459.39 °C, while PEBAX 1878 again underperformed the PIB-PA materials, experiencing its most significant mass loss at just 418.83 °C.

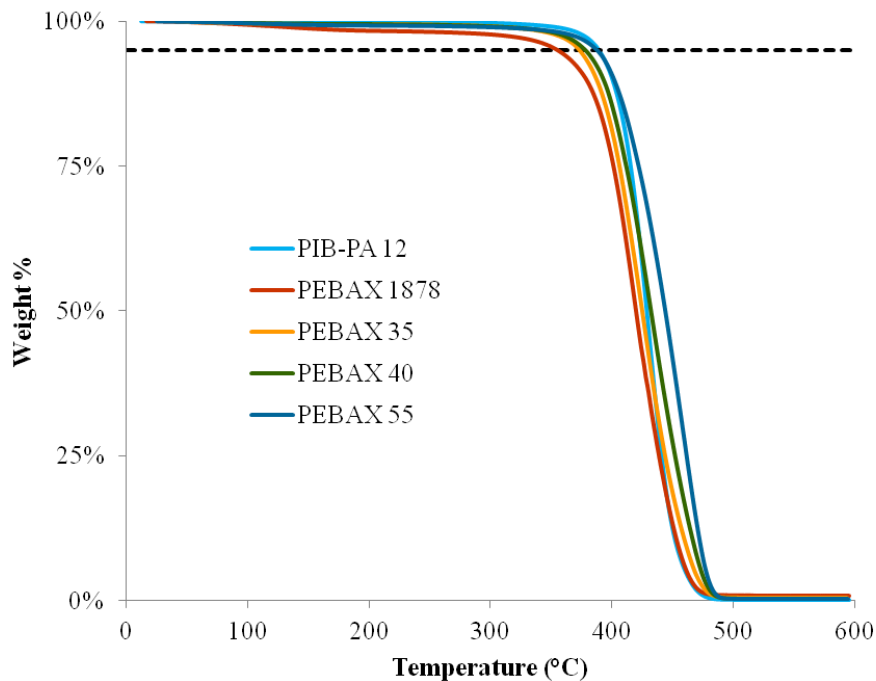


Figure 3.4 TGA thermogram comparison of Pebax<sup>®</sup> and representative PIB-PA TPEs.

The black dashed line marks 5% mass loss from the initial sample mass.

### 3.2.2 Differential Scanning Calorimetry (DSC)

DSC was used to examine the thermal behavior of the copolymers, particularly melt temperature ( $T_m$ ). Samples were heated to 280 °C to erase the thermal history of the material, then cooled to -80 °C and heated once more to 280 °C in order to observe any potential thermal transitions.

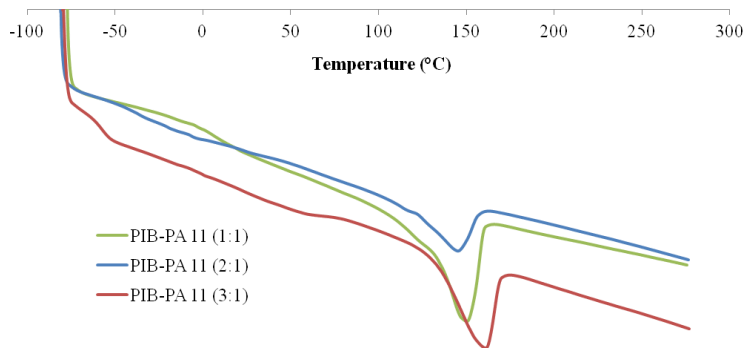


Figure 3.5 DSC thermogram comparison of PIB-PA 11 samples with varying weight ratios.

All samples represented are those utilizing PA of approximately 1,000 g/mol (for 1:1 and 2:1 samples, PA  $M_n$  = 1,020 g/mol; for 3:1 sample, PA  $M_n$  = 1,300 g/mol) with the appropriate molecular weight PIB to achieve the desired weight ratio. Samples targeting PIB:PA weight ratios of 1:1 and 2:1 were previously synthesized by Kucera, while the 3:1 sample was synthesized as described in Chapter II.

The second heating cycles for PIB-PA 11 samples of various targeted weight ratios are shown in Figure 3.5; the melting points and specific heat of fusion values found for each sample are reported in Table 3.2. The melting points all appear within a narrow range, as expected; they are determined by the hard blocks of the samples, which in this case are all PA-11 with molecular weights of approximately 1,000 g/mol. (The polyamide used for the 3:1 sample was slightly higher, around 1,300 g/mol, hence a slightly higher  $T_m$ .) The specific heat of fusion (amount of heat required to melt the sample on a mass

basis) also follows the trend one might expect: as the polyamide content decreases, the amount of energy needed (per gram) to melt the material also decreases.

Table 3.2

DSC data for PIB-PA 11 samples with varying weight ratios

Sample weight ratio (PIB:PA)	$T_m$ ( $^{\circ}\text{C}$ )	Specific heat of fusion (J/g)
1:1	150.35	82.12
2:1	145.64	54.85
3:1	161.70	34.80

All samples represented are those utilizing PA of approximately 1,000 g/mol (for 1:1 and 2:1 samples, PA  $M_n$  = 1,020 g/mol; for 3:1 sample, PA  $M_n$  = 1,300 g/mol) with the appropriate molecular weight PIB to achieve the desired weight ratio. Samples targeting PIB:PA weight ratios of 1:1 and 2:1 were previously synthesized by Kucera, while the 3:1 sample was synthesized as described in Chapter II. Specific heat of fusion values were taken as the integral of the melt peak in relation to the baseline of each respective curve.

Another interesting phenomenon can be noted between samples with the same targeted weight ratio of starting materials, but with different block lengths. The second DSC heat cycle for two different PIB-PA 11 samples with a targeted 3:1 PIB:PA weight ratio—one denoted the “shorter block” sample (synthesized with 3,400 g/mol PIB and 1,300 g/mol PA 11) and the other referred to as the “longer block” formulation (synthesized with 4,500 g/mol PIB and 1,430 g/mol PA-11)—can be seen in Figure 3.6. While the melting points appear to occur within roughly the same temperature range, the PIB-PA sample with longer hard and soft block lengths displays two melting peaks. There are multiple reasons for why a semicrystalline polymer might show multiple melting peaks, including polymorphism (the presence of multiple crystal structures).<sup>24</sup> Any crystallinity present in PIB-PA copolymers is due to the presence of the hard PA blocks, as they are able to form crystalline structures, unlike the amorphous PIB blocks.

It has been shown that polymer samples of lower molecular weight crystallize more easily, particularly for molecular weights less than 5,000 g/mol.<sup>25</sup> Double melting peaks might appear in the PIB-PA with longer block lengths due to the increased molecular weight of the PA block because longer chains are more susceptible to crystalline defects than shorter chains,<sup>26</sup> thus resulting in a distribution of melting peaks in the DSC thermogram.

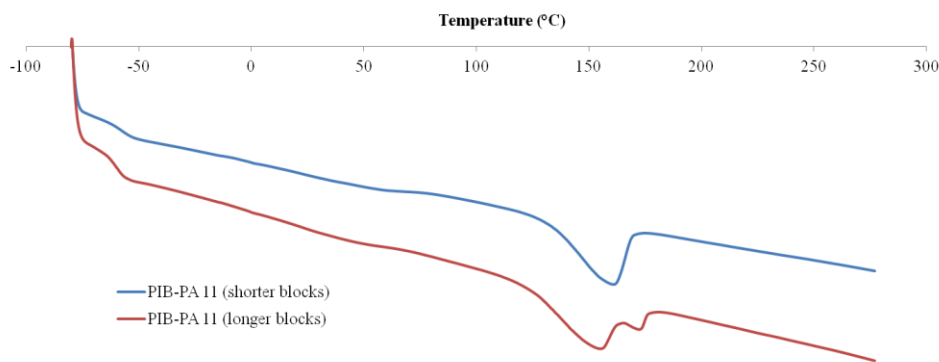


Figure 3.6 DSC thermogram comparison of 3:1 PIB-PA 11 samples with varying block lengths.

Both samples represented have targeted weight ratios of 3:1 PIB:PA. The “shorter block” sample is comprised of PIB with a molecular weight of approximately 3,400 g/mol and PA of approximately 1,300 g/mol, while the “longer blocks” sample is PIB and PA of approximately 4,500 and 1,500 g/mol, respectively.

The cooling and second heating cycles for all 3:1 PIB-PA samples can be seen in Figure 3.7, with thermal transitions of note displayed in Table 3.3. All samples display the same multiple-melting-peak behavior as seen above in Figure 3.6. Additionally, potential crystallization peaks are present in the samples, seen in the cooling portion of the heat cycle.



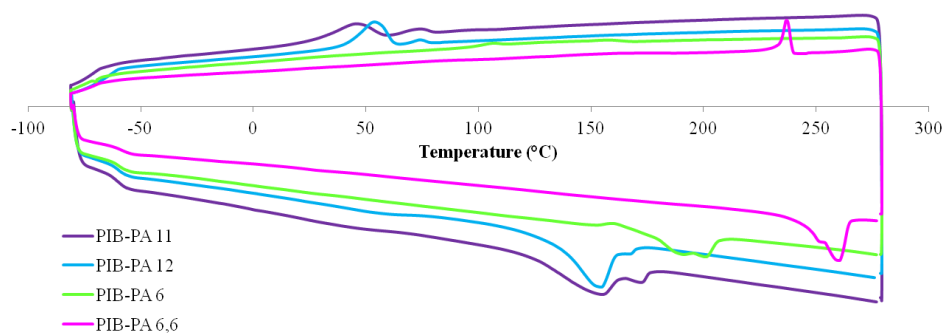


Figure 3.7 DSC thermogram comparison of 3:1 PIB-PA samples.

All PIB-PAs represented had a targeted PIB:PA weight ratio of 3:1, and originated from the same master batch of 4,500 g/mol PIB.

Table 3.3

Notable DSC transition temperatures for 3:1 PIB-PA samples

	Transition temperature (°C)		
	T <sub>g</sub>	T <sub>m</sub>	T <sub>c</sub>
PIB-PA 11	-60.68	159.02, 176.02	46.02, 74.37
PIB-PA 12	-59.83	154.50, 167.12	53.71, 74.04
PIB-PA 6	-59.88	191.47, 201.19	107.20, 157.84
PIB-PA 6,6	-58.42	251.55, 259.34	236.93

All samples represented are PIB-PA copolymers with a PIB:PA targeted weight ratio of 3:1, synthesized from the same master batch of 4,500 g/mol PIB.

All PIB-PA samples display a glass transition temperature of approximately -60 °C, due to the contribution of the PIB in the copolymers. The melting peaks for PIB-PA 11 and PIB-PA 12 appear in roughly the same range (centered around 160 °C). PIB-PA 6 melting peaks occur higher, around 195 °C, and PIB-PA 6,6 melting peaks occur highest of all, around 235 °C. This is expected, as a PA-6 or PA-6,6 block of the same length as a PA-11 or PA-12 block will contain more amide linkages per carbon atom in the backbone, producing stronger intermolecular forces. The higher melting temperature for

the PIB-PA 6,6 compared to the PIB-PA 6 TPE cannot be rationalized in terms of density of amide linkages, since the latter is essentially the same for these two polyamide hard blocks. According to literature, PA-6,6 produces crystals with a higher melting temperature because its structure enables easier and more favorable alignment of hydrogen bonding groups compared to PA-6.<sup>27</sup>

It is also noteworthy that PIB-PA 6,6 displays one sharp crystallization peak as opposed to the other PIB-PA samples, which show broad, multiple-peak behavior during the cooling cycle. This can again be attributed to the ability of PA-6,6 to form more uniform and more highly hydrogen-bonded structures of all the PA types investigated,<sup>28</sup> resulting in less variation in the transition temperatures displayed by the material. Surprisingly, the PIB-PA 6 sample shows crystallization peaks even broader than PIB-PA 11 and PIB-PA 12, to the extent that they are almost undetectable in the DSC thermogram. This suggests that the PA-6 segments of the copolymer did not crystallize to the expected degree.

### **3.2.3 Dynamic Mechanical Analysis (DMA)**

Dynamic mechanical analysis (DMA) was carried out on the PIB-PA copolymers in order to observe their viscoelastic behavior at varying temperatures and applied frequencies. This analysis allowed for observation of the  $T_g$  of the materials, as well as the storage modulus, loss modulus, and stiffness under differing conditions.

The first series of DMA experiments consisted of a temperature ramp from  $-80\text{ }^{\circ}\text{C}$  to  $100\text{ }^{\circ}\text{C}$  at a constant frequency of 1 Hz. A plot of  $\tan \delta$  versus temperature, as shown in Figure 3.8, allows some insight into the elastic behavior of the material over the given temperature range.  $\tan \delta$  represents a ratio of loss modulus (dissipated energy) over

storage modulus (recoverable energy), meaning that higher  $\tan \delta$  values imply more viscous material behavior. A peak in the  $\tan \delta$  curve can also correspond to a glass transition temperature, as it represents a point where the material is becoming more flexible as viscous behavior becomes more prominent than elastic behavior. In the case of PIB, a bimodal  $\tan \delta$  peak is typically observed, with the  $T_g$  (related to local segmental motions) appearing as a shoulder on the low-temperature side of a more intense, sub-Rouse relaxation (related to larger-scale segmental motions).<sup>29</sup>

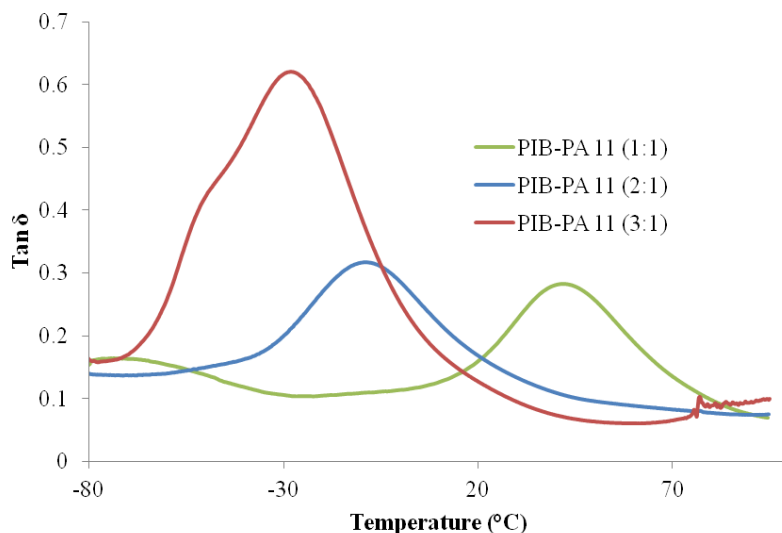


Figure 3.8 DMA temperature ramp of PIB-PA 11 samples with varying weight ratios.

All samples represented are those utilizing PA of approximately 1,000 g/mol (for 1:1 and 2:1 samples, PA  $M_n = 1,020$  g/mol; for 3:1 sample, PA  $M_n = 1,300$  g/mol) with the appropriate molecular weight PIB to achieve the desired weight ratio. Samples targeting PIB:PA weight ratios of 1:1 and 2:1 were previously synthesized by Kucera, while the 3:1 sample was synthesized as described in Chapter II. The temperature ramp was conducted at a constant frequency of 1 Hz.

The 3:1 sample in Figure 3.8 shows the above-discussed bimodal  $\tan \delta$  peak typical of PIB, consisting of a  $T_g$  around  $-50$  °C and a higher-temperature, higher-intensity sub-Rouse relaxation. Other than a very weak shoulder at  $13$  °C, this sample does not display any relaxations characteristic of PA-11. The 2:1 sample, which is

compositionally lower in PIB, still appears to show a weak PIB  $T_g$  around  $-50\text{ }^\circ\text{C}$ , but the sub-Rouse relaxation has been replaced by a new relaxation centered at about  $-8\text{ }^\circ\text{C}$ , which we have tentatively assigned to a  $T_g$  of a PA-rich mixed PIB-PA phase. The 1:1 sample, which is compositionally lowest in PIB, shows a prominent relaxation at  $42\text{ }^\circ\text{C}$ , which is near the reported  $T_g$  of PA-11 ( $43\text{ }^\circ\text{C}$ ).<sup>7</sup> This sample does not display a PIB  $T_g$  at  $-50\text{ }^\circ\text{C}$  but rather a broad sub- $T_g$  peak of relatively low intensity centered about  $-75\text{ }^\circ\text{C}$ . In general, at larger PIB contents (the 3:1 sample) the smaller PA blocks are partially or mostly incorporated into the larger PIB phases causing the  $\tan\delta$  to be entirely dominated by the PIB phases, whereas the opposite is true at larger PA contents. The intensity of the dominant peak also increases with increasing PIB content; this trend agrees with the idea that a higher ratio of PIB present in the copolymer will more closely align the material's properties with that of pure PIB, which would perform more as a viscous material than an elastic one without the addition of hard PA blocks. A higher PIB content also means an amplified sub-Rouse relaxation effect in relation to lower PIB content samples, contributing to a higher primary  $\tan\delta$  peak.

Utilizing longer blocks of both precursors also increases the damping behavior of the material, according to the  $\tan\delta$  curves for 3:1 PIB-PA 11 samples with varying block lengths as shown in Figure 3.9. Similar to the behavior seen in Figure 3.8, both peaks show a lower-temperature shoulder around  $-50\text{ }^\circ\text{C}$ , indicating that block length does not have an effect on the  $T_g$  of the PIB-PA. However, the primary  $\tan\delta$  peak for the sample with longer blocks is significantly higher than that of its shorter-block counterpart. This could be due to more intense Rouse relaxation behavior in the higher molecular weight PIB blocks, providing a more intense  $\tan\delta$  response, and therefore making the  $T_g$

shoulder appear more prominently on the curve representing the PIB-PA sample with lower molecular weight blocks.

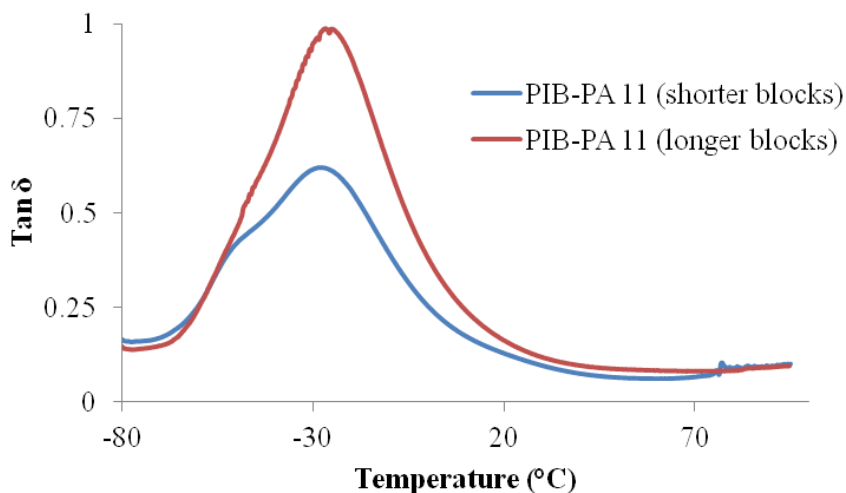


Figure 3.9 DMA temperature ramp of 3:1 PIB-PA 11 samples with varying block lengths.

Both samples represented have targeted weight ratios of 3:1 PIB:PA. The temperature ramp was conducted at a constant frequency of 1 Hz.

Figure 3.10 compares  $\tan \delta$  values versus temperature for 3:1 PIB-PA materials synthesized using a variety of types of PA. The maximum  $\tan \delta$  value appears at roughly the same temperature for all PIB-PA types, as opposed to the differing peak positions observed in Figure 3.8; this suggests that the fraction of PIB present in the material is likely the main factor in determining the  $T_g$  of the material, with little to no influence coming from the type of PA that is selected. The elastic behavior of the material at a given temperature is still affected by the PA type, however. PIB-PA 6,6 displays the lowest  $\tan \delta$  maximum, as expected; it uses the most robust PA of the varieties examined, meaning that the hard blocks of PA-6,6 will be most successful at offsetting the more viscous behavior of the PIB soft blocks. PIB-PA 11 and PIB-PA 12 display very similar  $\tan \delta$  behavior, which is expected, since they differ by just one carbon atom in the PA

hard block backbone. PIB-PA 6, however, unexpectedly displays the highest  $\tan \delta$  values, meaning that of all the PIB-PA varieties investigated, it performed the most similarly to pure PIB. This behavior matches with the observations made in the discussion of the DSC thermogram seen in Figure 3.7; if the PA-6 hard blocks did not crystallize to a high extent, the overall material would behave more like pure PIB than the other TPEs synthesized.

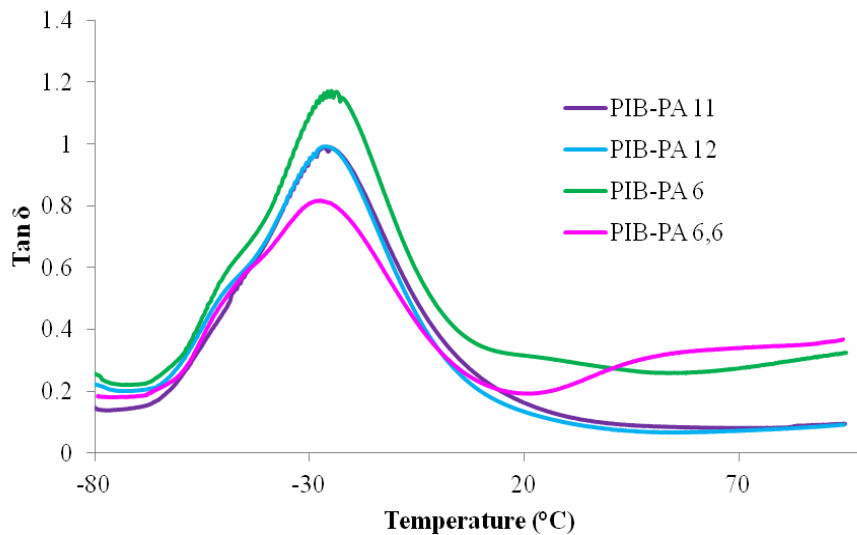


Figure 3.10 DMA temperature ramp of 3:1 PIB-PA samples.

All samples represented are PIB-PA copolymers with a PIB:PA targeted weight ratio of 3:1, synthesized from the same master batch of 4,500 g/mol PIB. The temperature ramp was carried out at a constant frequency of 1 Hz.

A comparison can also be made between the synthesized PIB-PA samples and the commercial standard Pebax<sup>®</sup> TPEs. A plot of  $\tan \delta$  values collected during a DMA temperature ramp for the four grades of Pebax<sup>®</sup> as well as a representative PIB-PA sample (PIB-PA 12) can be seen in Figure 3.11. PIB-PA 12 displays dramatically higher  $\tan \delta$  values at lower temperatures; this is consistent with the well-known, high mechanical damping characteristics of PIB in the lower temperature range. The inset plot of Figure 3.11 displaying solely the  $\tan \delta$  curves of the Pebax<sup>®</sup> materials shows that they

display secondary peaks at higher temperatures rather than shoulders on their primary peaks as PIB-PA 12 does, suggesting that phase separation may be greater in these TPEs than in PIB-PA materials.

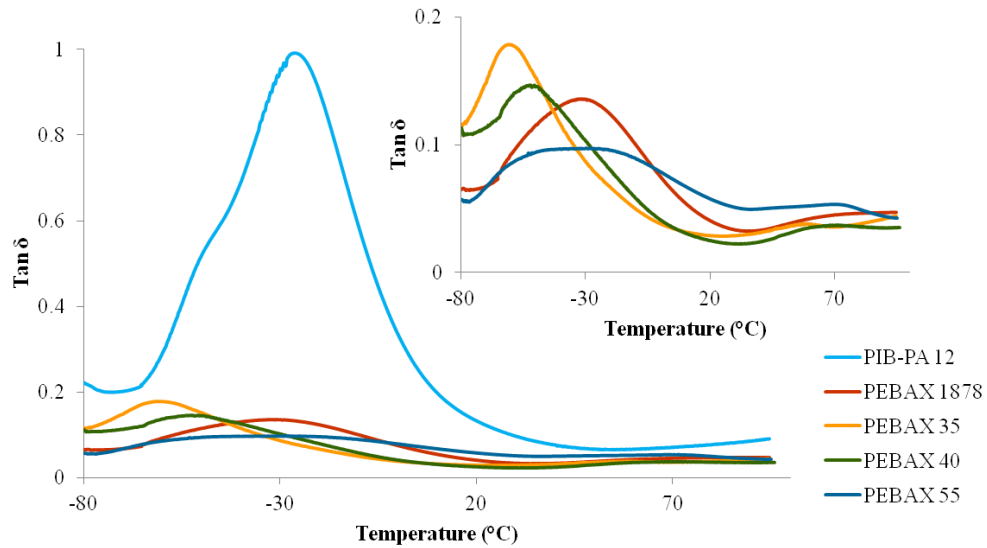


Figure 3.11 DMA temperature ramp of Pebax® and representative PIB-PA TPEs.

Experiments were performed at a constant 1 Hz. The main plot includes a representative PIB-PA sample (PIB-PA 12), while the inset plot shows solely the Pebax® materials.

The second series of DMA experiments carried out was a frequency sweep from 1 Hz to 200 Hz while the sample was held isothermally at 25 °C. Such an experiment is useful for predicting the behavior of a material in an application where it might experience varying stress loads under ambient conditions. For example, athletic shoe soles must be able to respond to high force impacts experienced during running as well as lower stresses seen during walking, the intensity of which will also vary between users. Figure 3.12 shows a comparison in the stiffness values (where stiffness represents the force applied to the material divided by the amplitude of deformation) of PIB-PA 11 samples with varying weight ratios of PIB:PA. The PIB-PA 11 sample with the highest

fraction of PA (the 1:1 sample) is shown to be the stiffest, with stiffness decreasing as the PA content of the formulations is decreased. This is as we might expect; increasing the PIB content of the sample increases the flexibility, as the PIB soft block is the elastic contributor to the copolymer.

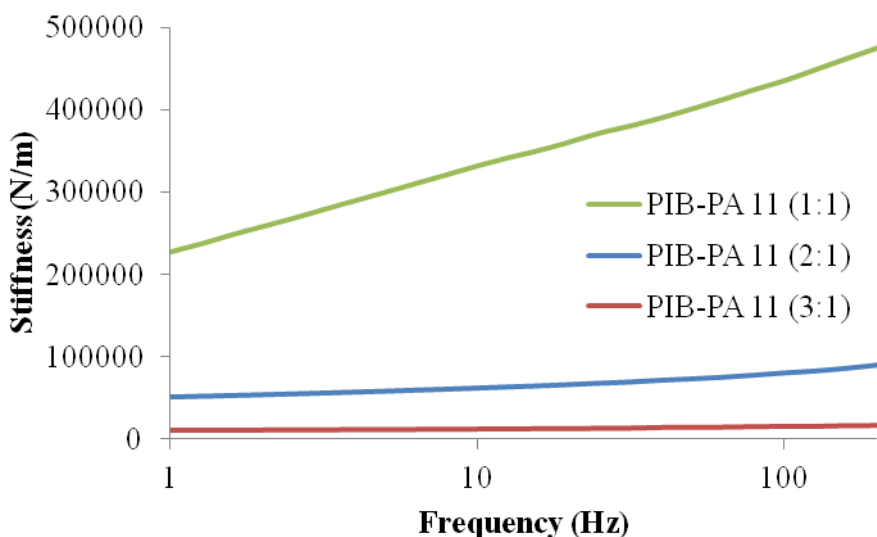


Figure 3.12 DMA room temperature frequency sweep of PIB-PA 11 samples with varying weight ratios.

All samples represented are those utilizing PA of approximately 1,000 g/mol (for 1:1 and 2:1 samples, PA  $M_n = 1,020$  g/mol; for 3:1 sample, PA  $M_n = 1,300$  g/mol) with the appropriate molecular weight PIB to achieve the desired weight ratio. Samples targeting PIB:PA weight ratios of 1:1 and 2:1 were previously synthesized by Kucera, while the 3:1 sample was synthesized as described in Chapter II. Note that frequency is displayed on a log scale.

A change in behavior can also be witnessed when the block lengths are varied in different samples of PIB-PA 11. Figure 3.13 shows a comparison of the stiffness of two samples of PIB-PA 11 with the same 3:1 weight ratio of PIB:PA, but comprised of hard and soft blocks of differing molecular weights. The sample with shorter block lengths is stiffer than its longer-block counterpart at any given frequency, as the longer chains provide more flexibility to the material during applied deformation. Both materials display a fairly linear trend in their stiffness values up to approximately 30 Hz, at which



point the stiffness becomes slightly more unpredictable; however, because the scatter is still centered around a general linear trend, this is thought to be instrument noise amplified due to the harsher test conditions being experienced (higher frequencies). Additionally, increasing frequency seems to have more of an influence on the stiffness of the shorter block sample, as the stiffness trend in the longer block sample remains more consistent across the tested frequency range.

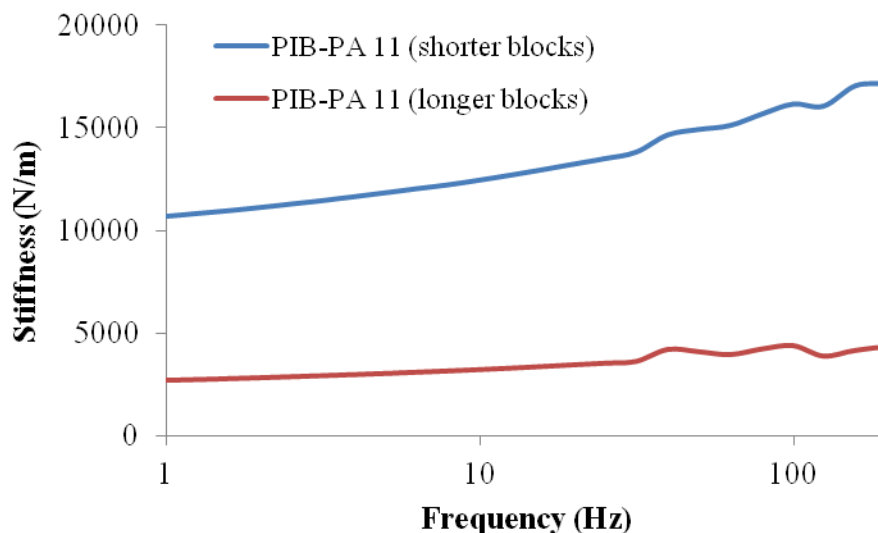


Figure 3.13 DMA room temperature frequency sweep of 3:1 PIB-PA 11 samples with varying block lengths.

The “shorter blocks” sample is a PIB-PA 11 formulation consisting of PIB with a molecular weight of approximately 3,400 g/mol and PA of approximately 1,300 g/mol, while the “longer blocks” sample is PIB and PA of approximately 4,500 and 1,500 g/mol, respectively. Note that the frequency is displayed on a log scale.

Finally, Figure 3.14 compares the stiffness values of 3:1 PIB-PA materials prepared from the four different types of PA blocks, over a frequency range of 1 to 200 Hz. Again, all the materials show smooth curves up to approximately 30 Hz, at which point the curves begin to deviate but still maintain a fairly linear trend. Unsurprisingly, PIB-PA 6,6 shows the highest stiffness values at any frequency, as it was synthesized

with the stiffest PA hard block of the formulations tested. Consistent with the  $\tan \delta$  versus temperature data presented earlier in Figure 3.10, once again, PIB-PA 6 displays the lowest stiffness values of any of the PIB-PA samples. This further supports the thought that the hard blocks within PIB-PA 6 did not crystallize to the greater extent expected of them over the hard blocks of PIB-PA 11 and PIB-PA 12, resulting in behavior more similar to that of pure PIB than the other TPEs.

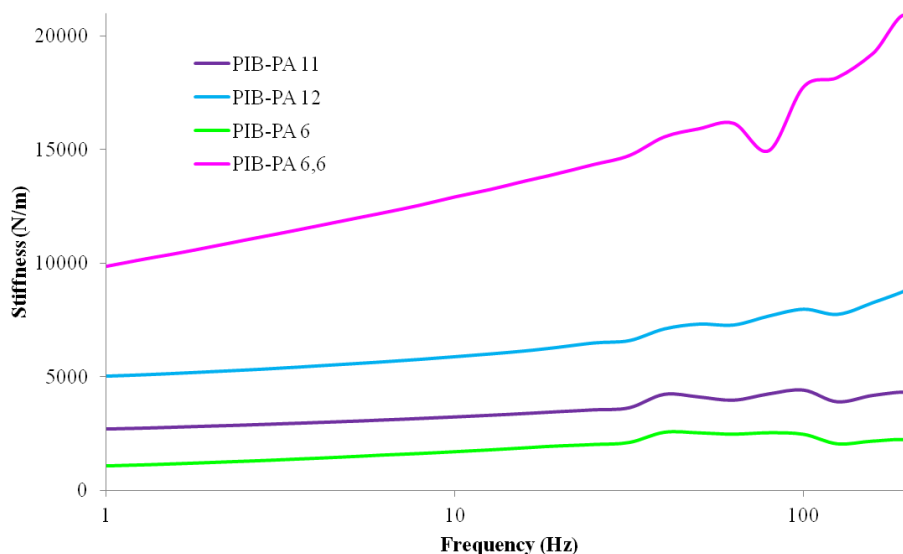


Figure 3.14 DMA room temperature frequency sweep of 3:1 PIB-PA samples.

All samples represented are PIB-PA copolymers with a PIB:PA targeted weight ratio of 3:1, synthesized from the same master batch of 4,500 g/mol PIB.

Room temperature frequency sweeps were also carried out on Pebax<sup>®</sup> TPEs for comparison to the PIB-PA materials. The Pebax<sup>®</sup> materials consistently showed greater stiffness values than PIB-PA copolymers across any frequency applied to the materials, as shown in Figure 3.15. This is consistent with the  $\tan \delta$  versus temperature data in Figure 3.11. The curves of Figure 3.15 show the same instrumental noise above 30 Hz that was observed for the PIB-PA samples in the previous figures. This phenomenon is

especially visible in the magnified view of the stiffness data for PEBAX 35 seen in the inset plot of Figure 3.15.

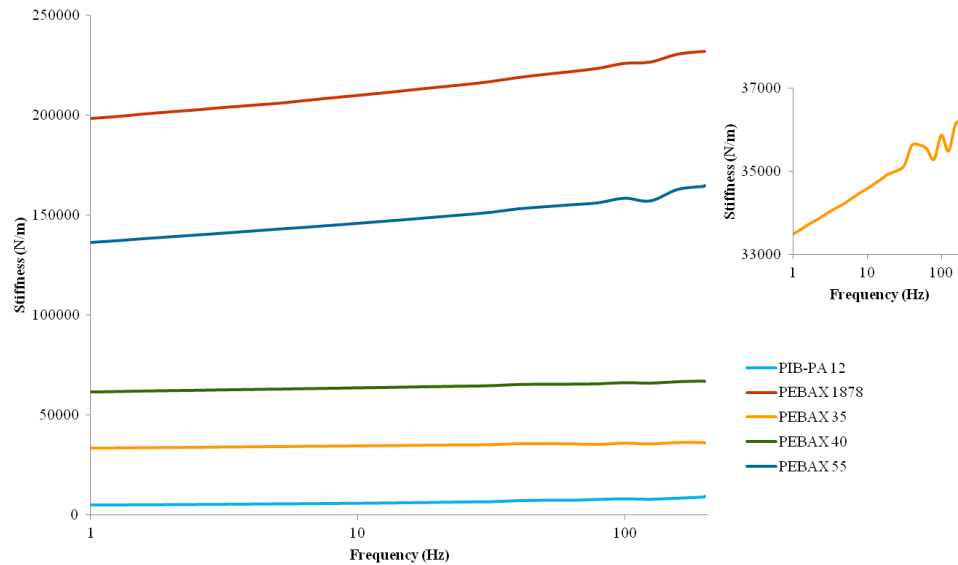


Figure 3.15 DMA room temperature frequency sweep of Pebax<sup>®</sup> and representative PIB-PA TPEs.

All experiments were run at a constant 25 °C. The main plot includes a representative PIB-PA sample (PIB-PA 12), while the inset plot displays a magnified view of solely the PEBAX 35 stiffness curve.

The third and final DMA profile collected was a frequency sweep-temperature step experiment, covering temperatures in the range of -20 °C to 80 °C and frequencies from 1 to 200 Hz. Such an experiment probes material behavior over a wider variety of environmental changes. A comparison of the stiffness values collected during these experiments for PEBAX 35 and PIB-PA 12 are shown in Figure 3.16. Both materials show a decrease in stiffness as the temperature of the furnace was increased. However, PIB-PA 12 showed overall more consistent stiffness behavior between temperature increments than PEBAX 35. Alternatively, increasing frequency had a greater effect on PIB-PA 12, especially at lower temperatures (-20 and 0 °C) than on PEBAX 35.

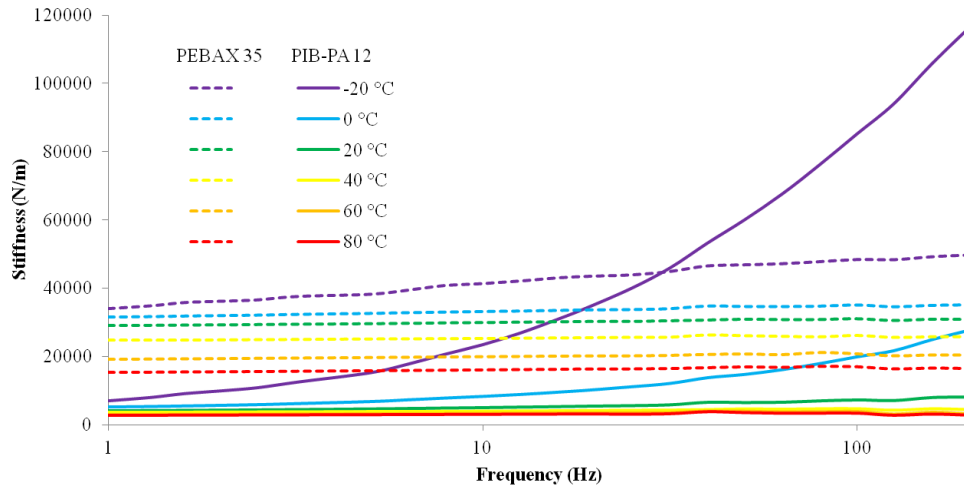


Figure 3.16 DMA frequency sweep-temperature step comparison of PEBAX 35 and PIB-PA 12.

Different temperatures are represented by the given colors, while the line type differentiates between PEBAX 35 (dashed lines) and PIB-PA 12 (solid lines).

### 3.2.4 Tensile Testing

Certain mechanical properties of PIB-PA were investigated via tensile testing.

Extension-to-break was performed to generate information regarding the elastic behavior of the materials such as elastic modulus, tensile strength, and elongation to break.

Tension set testing was also carried out on PIB-PA and Pebax<sup>®</sup> materials to investigate the recoverability of the TPEs after deformation.

The first structure-property relationship to be elucidated was the effect of the PIB:PA weight ratio on the mechanical behavior of the copolymer. PIB-PA 11 samples with three different ratios of PIB:PA were formed into dumbbell bars and subjected to an extension-to-break experiment as shown in Figure 3.17; the data shown consist of a representative curve for each grade of PIB-PA 11, chosen from the multiple specimens tested. Average modulus, peak stress, and strain at break values for the different samples are listed in Table 3.4.

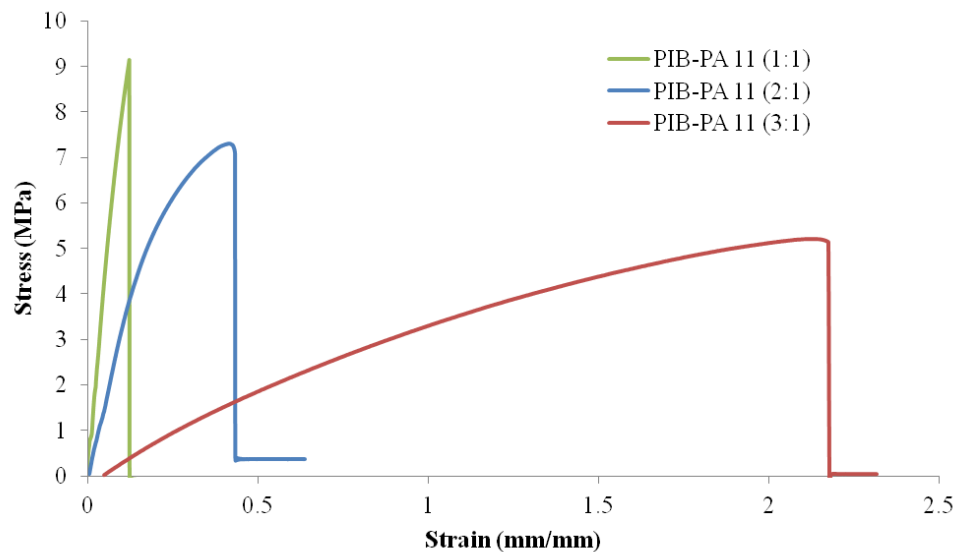


Figure 3.17 Representative stress-strain curves for PIB-PA 11 samples with varying weight ratios.

All samples represented are those utilizing PA of approximately 1,000 g/mol (for 1:1 and 2:1 samples, PA  $M_n$  = 1,020 g/mol; for 3:1 sample, PA  $M_n$  = 1,300 g/mol) with the appropriate molecular weight PIB to achieve the desired weight ratio. Samples targeting PIB:PA weight ratios of 1:1 and 2:1 were previously synthesized by Kucera, while the 3:1 sample was synthesized as described in Chapter II.

Table 3.4

Mechanical properties of PIB-PA 11 samples with varying weight ratios

Weight ratio (PIB:PA)	Modulus (MPa)	Peak Stress (MPa)	Strain at Break (mm/mm)
1:1	101.681	8.957	0.103
2:1	34.633	6.808	0.372
3:1	4.515	5.314	2.013

All samples represented are those utilizing PA of approximately 1,000 g/mol (for 1:1 and 2:1 samples, PA  $M_n$  = 1,020 g/mol; for 3:1 sample, PA  $M_n$  = 1,300 g/mol) with the appropriate molecular weight PIB to achieve the desired weight ratio. Samples targeting PIB:PA weight ratios of 1:1 and 2:1 were previously synthesized by Kucera, while the 3:1 sample was synthesized as described in Chapter II. Values shown are averages of all specimens tested

As expected, the material behaved more elastically as the PIB content of the copolymer was increased. The 1:1 PIB-PA copolymer acted as a more brittle material, displaying a sharp peak giving a high modulus value before fracturing after minimal extension. The 2:1 PIB-PA showed a slower initial rise in stress in relation to extension before break, resulting in lower modulus and peak stress values. The trend continued with the increase to a 3:1 weight ratio of PIB:PA; the most PIB-dominant of the three samples on average underwent a much longer extension before break than the other tested ratios, resulting in an even lower modulus. Lengthening the PIB blocks in relation to a static PA block length introduces more flexibility into the copolymer. The flexible PIB chains are able to extend more easily than their PA counterparts during testing, allowing the material to withstand more strain at higher PIB contents. This results in a much higher toughness—defined as the ability of a material to undergo deformation before reaching the point of fracture, and represented as the area under the stress-strain curve. Alternatively, an increased PA content will provide for a stiffer material, resulting in an increase in the Young's modulus of the copolymer.

A comparison between PIB-PAs using starting materials of the same PA type and the same target weight ratio but with differing block lengths was also performed. Two different samples of PIB-PA 11 with weight ratios of 3:1 PIB:PA were subjected to tensile testing; the first was prepared from 3,400 g/mol PIB and 1,300 g/mol PA, and the second from 4,500 g/mol PIB and 1,500 g/mol PA. An overlay of representative stress-strain curves can be seen in Figure 3.18, with accompanying mechanical property data found in Table 3.5. The sample with longer blocks of both starting materials was able to undergo a higher strain before fracturing, confirming that absolute block length

influences mechanical properties, in addition to the hard:soft block length ratio. Longer PA chains allow for the hard block of the material to become more flexible than the same material at a shorter chain length, thus leading to a decreased Young’s modulus (indicative of more elastic behavior).

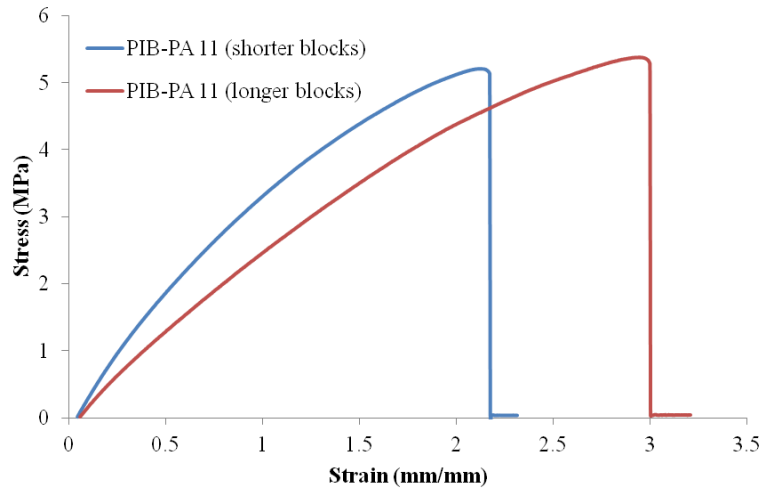


Figure 3.18 Representative stress-strain curves for 3:1 PIB-PA 11 samples with varying block lengths.

The “shorter blocks” sample is a PIB-PA 11 formulation consisting of PIB with a molecular weight of approximately 3,400 g/mol and PA of approximately 1,300 g/mol, while the “longer blocks” sample is comprised of PIB and PA of approximately 4,500 and 1,500 g/mol, respectively.

Table 3.5

Mechanical properties of 3:1 PIB-PA 11 samples with varying block lengths

Sample	Modulus (MPa)	Peak Stress (MPa)	Strain at Break (mm/mm)
PIB-PA 11 (Shorter blocks)	4.515	5.314	2.013
PIB-PA 11 (Longer blocks)	2.475	5.265	2.954

The “shorter blocks” sample is a PIB-PA 11 formulation consisting of PIB with a molecular weight of approximately 3,400 g/mol and PA of approximately 1,300 g/mol, while the “longer blocks” sample is comprised of PIB and PA of approximately 4,500 and 1,500 g/mol, respectively. All values displayed are averages gathered from all specimens tested per sample type.

Finally, the effect of the different PA varieties utilized in the PIB-PA copolymers was studied. PIB-PA samples utilizing four different types of PA underwent extension-to-break tensile testing, stress-strain curves for which are shown in Figure 3.19.

Accompanying tensile property data for these materials can be found in Table 3.6.

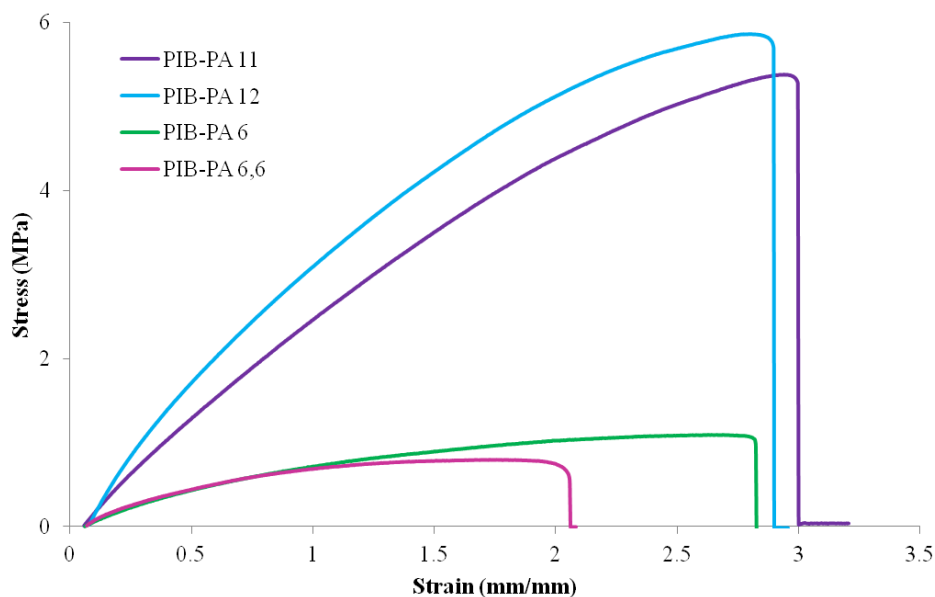


Figure 3.19 Representative stress-strain curves for 3:1 PIB-PA samples.

All samples represented are PIB-PA copolymers with a PIB:PA targeted weight ratio of 3:1, synthesized from the same master batch of 4,500 g/mol PIB.



Table 3.6

Mechanical properties of 3:1 PIB-PA and Pebax<sup>®</sup> TPEs

Sample	Modulus (MPa)	Peak Stress (MPa)	Strain At Break (mm/mm)
PIB-PA 11	2.475	5.265	2.954
PIB-PA 12	3.345	5.984	2.862
PIB-PA 6	0.774	1.196	3.367
PIB-PA 6,6	1.163	0.889	1.865
PEBAX 35	10.542	8.086	6.271
PEBAX 40	22.923	13.388	---
PEBAX 55	40.225	17.971	---
PEBAX 1878	35.151	19.596	2.850

All values displayed are averages gathered from all specimens tested per sample type. PEBAX 40 and PEBAX 55 did not experience fracture before samples experienced slippage from the instrument's grips.

The samples with longer PA repeat units (PIB-PA 11 and PIB-PA 12) reach much greater peak stress values before failure than the formulations utilizing shorter PA types (PIB-PA 6 and PIB-PA 6,6). PA-11 and PA-12 are more flexible hard blocks as they contain longer aliphatic chains between amide linkages, allowing them to extend more easily than PA-6 or PA-6,6. This makes PIB-PA 11 and PIB-PA 12 tougher materials, allowing them to undergo greater deformation prior to break. PIB-PA 6 again showed somewhat unexpected behavior, as it displayed a longer average strain at break than PIB-PA 11 and PIB-PA 12. This observation supports the earlier conclusion that the PA segments did not crystallize to the degree expected, causing the material to display more PIB-like properties than the other PIB-PA varieties examined.

Increasing the PIB content in PIB-PA copolymers produced materials that perform more like Pebax<sup>®</sup> TPEs. For example, the 3:1 PIB:PA samples displayed twenty-fold higher strain at break values compared to 2:1 or 1:1 PIB:PA samples, enabling them

to elongate to the same extent as some Pebax<sup>®</sup> grades, as shown in Figure 3.20.

Alternatively, the lower-PIB-content PIB-PA samples performed similarly to Pebax<sup>®</sup> in terms of modulus, as reported in Table 3.4 and Table 3.6.

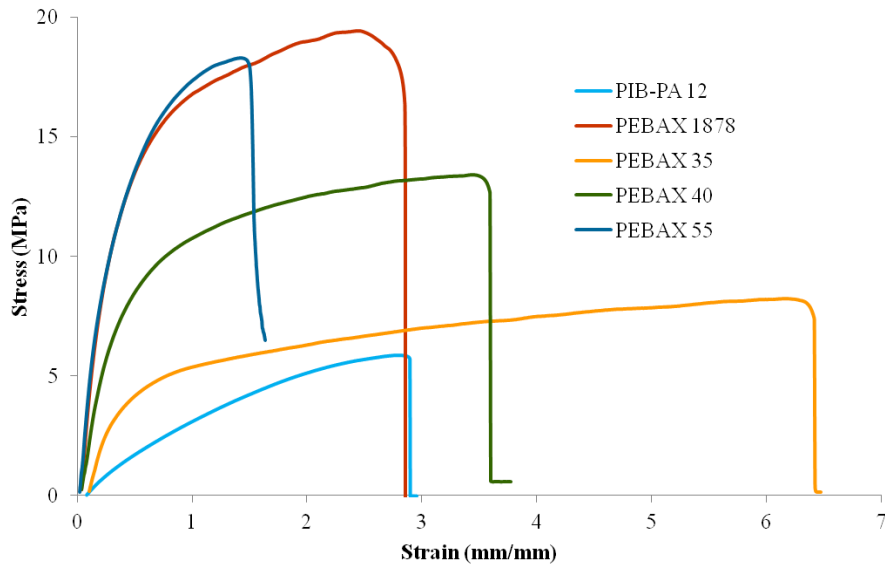


Figure 3.20 Representative stress-strain curves of Pebax<sup>®</sup> and representative PIB-PA TPEs.

Tension set (also referred to as “permanent set”) testing was also carried out on the TPEs. Dumbbell bars were marked, measured, extended 25 mm, held for 10 min, then released and allowed to recover. After a 10 min recovery period, the percent elongation of the material between benchmarks as compared to the initial benchmark length was calculated, and is reported in Table 3.7.

Table 3.7

Tension set results for PIB-PA and Pebax<sup>®</sup> TPEs

Sample	Elongation (%)
PIB-PA 11	6.87
PIB-PA 12	---
PIB-PA 6	10.03
PIB-PA 6,6	---
PEBAX 35	47.73
PEBAX 40	76.15
PEBAX 55	164.56

Elongation percentages given are relative to the initial length of the measured benchmarks. Values displayed are averages of all specimens tested for each sample type. All PIB-PA 12 and PIB-PA 6,6 samples broke before the conclusion of the 10 min extension period.

The PIB-PA samples that successfully underwent the tension set experimentation displayed excellent recoverability. PIB-PA 11, for example, only showed an average post-extension increase in length of 6.87%. The Pebax<sup>®</sup> samples displayed larger permanent changes in length: PEBAX 35 was the best performing of the commercial grades in this aspect, showing an average tension set extension of about 48%, while PEBAX 55 was the most permanently deformed of the materials, maintaining a post-test extension of about 165% of that of its original length. This means that PIB-PA could be a more viable option for applications in which recoverability after slight deformation, such as expansion and contraction of gasket seals, is a necessary TPE quality. However, more investigation must be made into what formulation adjustments are necessary in order to ensure that PIB-PA samples survive the 10 min extension period of the tension set testing, as this is where Pebax<sup>®</sup> outperformed the PIB-PA TPEs. All PIB-PA 12 and PIB-PA 6,6 samples successfully underwent the initial extension, but experienced clean breaks along the narrow section of the dumbbell shape approximately 5 min into the

extension-hold portion of the test. No necking was evident, suggesting that failure could be due to propagation of an internal void created during melt press preparation of the specimens rather than the inability of the polymer chains to extend to longer conformations. More samples could be tested in order to confirm this explanation.

### **3.3 Conclusions**

Overall, marked improvements were made to some aspects of the mechanical and thermal properties of PIB-PA materials as compared to samples previously synthesized by Kucera through a variety of adjustments, including an increase of the PIB content in their formulations, an increase in the molecular weight of both the soft and hard blocks, the utilization of mechanical stirring during copolymerization, and the introduction of new varieties of PA as the hard block. Larger molecular weights were hinted at, likely due to mechanical stirring, giving hope to improved mechanical properties that were eventually witnessed. An increase in melting point was seen, especially when PA-6,6 was chosen to serve as the hard block in the copolymer. Increasing PIB content increased the strain capabilities of PIB-PA during tensile testing, making it able to withstand much more deformation before fracture (increased toughness). Similar improvements were seen when overall block length was increased for both the soft and hard blocks as well.

However, Pebax<sup>®</sup> did continue to outperform PIB-PA in some aspects. Pebax<sup>®</sup> remains an overall tougher material as witnessed during tensile testing, so more adjustments to the PIB-PA formulation must be made. This could include further increasing the block length of both the PIB and PA blocks, and possibly using extrusion as a method to further improve mixing of the PIB and PA during copolymerization. Investigating these potential paths to better mechanical properties could allow us to

determine if PIB-PA can serve as a suitable replacement for Pebax<sup>®</sup> materials, or whether the structure of PIB simply doesn't allow for as strong mechanical properties in the resultant TPE as other soft blocks choices, such as PTMO<sup>30</sup> or PEO.

Other future work to be done in order to learn more about the structure-property relationships of this class of TPE could include atomic force microscopy (AFM), which could give more insight to the phase-separation behavior of PIB-PA. With continued improvements, PIB-PA copolymers could become a viable option for a variety of applications on the TPE market.

## APPENDIX A – Supplementary Figures and Tables

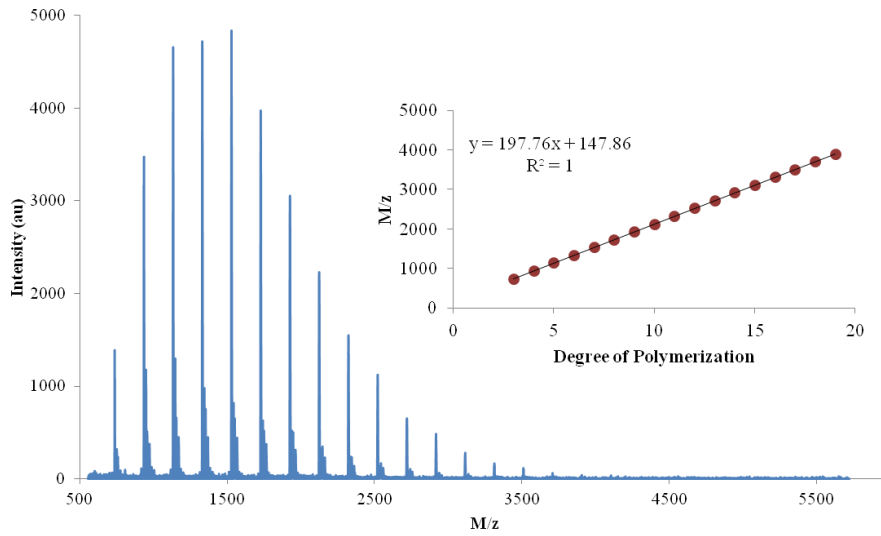


Figure A.1 MALDI-TOF MS spectrum for PA-12.

The peaks of the large plot (showing intensity vs. mass/charge ratio) were used to construct the inset plot, which shows mass/charge ratio vs. degree of polymerization and allows the calculation of repeat unit and end group masses.

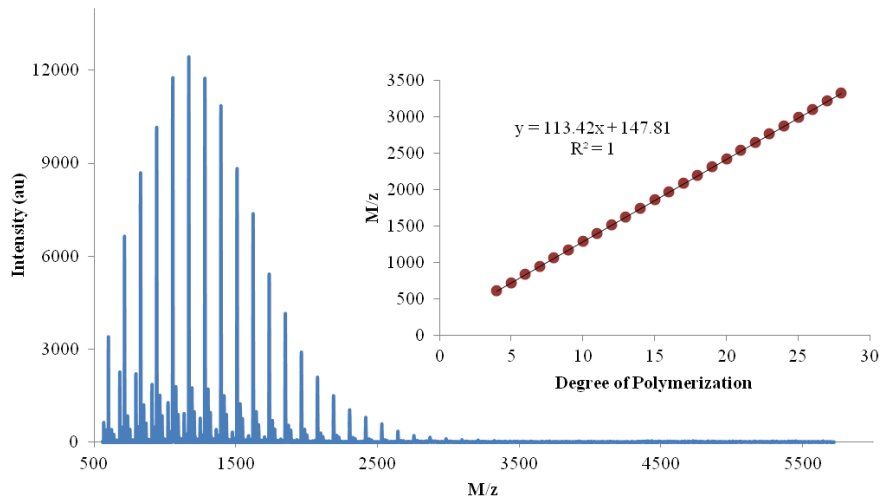


Figure A.2 MALDI-TOF MS spectrum for PA-6.

The peaks of the large plot (showing intensity vs. mass/charge ratio) were used to construct the inset plot, which shows mass/charge ratio vs. degree of polymerization and allows the calculation of repeat unit and end group masses.

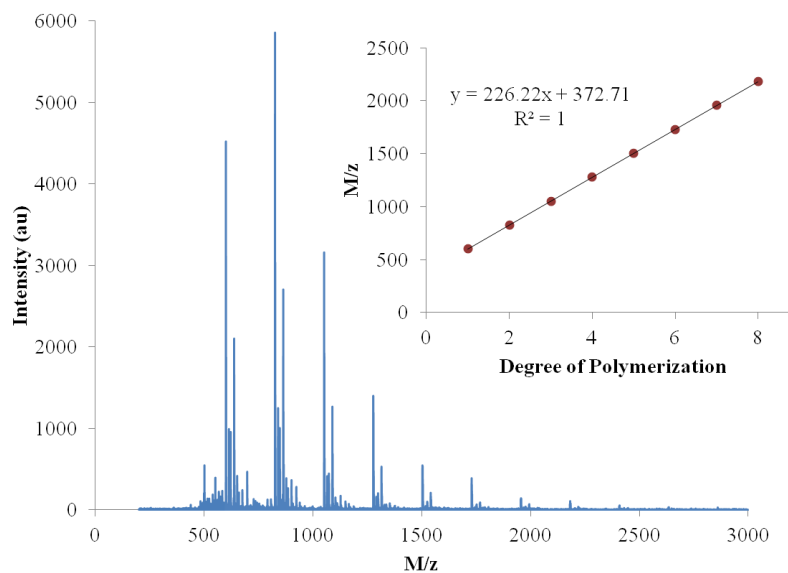


Figure A.3 MALDI-TOF MS spectrum for PA-6,6.

The peaks of the large plot (showing intensity vs. mass/charge ratio) were used to construct the inset plot, which shows mass/charge ratio vs. degree of polymerization and allows the calculation of repeat unit and end group masses.

Table A.1

Polyamide MALDI-TOF MS molecular weight experimental and theoretical comparison

Polyamide	Repeat unit mass (g/mol)		End group mass (g/mol)	
	Expected	Experimental	Expected	Experimental
PA-11	183.30	183.70	146.14	146.96
PA-12	197.32	197.76	146.14	147.86
PA-6	113.16	113.42	146.14	147.81
PA-6,6	226.32	226.22	372.46	372.71

The expected repeat unit mass given is based on the repeating unit (also accounting for water loss) of each polymer: 11-aminoundecanoic acid for PA-11, 12-aminododecanoic acid for PA-12,  $\epsilon$ -caprolactam for PA-6, and one unit each of adipic acid and 1,6-hexanediamine for PA-6,6. The expected end group mass is one unit of adipic acid for all polymers, except in the case of PA-6,6: because the degree of polymerization count in the MALDI-TOF MS analysis began at 2, the end group molecular weight value here includes one repeat unit of the polymer as well as an additional unit of adipic acid.

## REFERENCES

- (1) Snyder, M. D. Elastic Copolyesters and Process. US Patent 2,623,033, 1952.
- (2) Drobny, J. G. *Handbook of Thermoplastic Elastomers*; William Andrew Inc.: Norwich, NY, 2007.
- (3) Chen, A. T.; Farrissey, W. J.; Nelb, R. G. Polyester Amides Suitable for Injection Molding. 4,129,715, 1978.
- (4) Deleens, G.; Foy, P.; Jungblut, C. Moldable And/or Extrudable Polyether-Ester-Amide Block Copolymers. US Patent 4,331,786, 1980.
- (5) Malet, F. L. G. Thermoplastic Poly(Ether-B-Amide) Elastomers: Synthesis. In *Handbook of Condensation Thermoplastic Elastomers*; Fakirov, S., Ed.; 2005.
- (6) Jewrajka, S. K.; Yilgor, E.; Yilgor, I.; Kennedy, J. P. Polyisobutylene-Based Segmented Polyureas. I. Synthesis of Hydrolytically and Oxidatively Stable Polyureas. *J. Polym. Sci. Part A Polym. Chem.* **2009**, *47*, 38–48.
- (7) *Polymer Handbook*; Brandrup, J., Immergut, E. H., Eds.; John Wiley & Sons, Inc., 1975.
- (8) Ojha, U.; Rajkhowa, R.; Agnihotra, S. R.; Faust, R. A New General Methodology for the Syntheses of End-Functional Polyisobutylenes by Nucleophilic Substitution Reactions. *Macromolecules* **2008**, *41* (11), 3832–3841.
- (9) Kennedy, J. P.; Smith, R. A. New Telechelic Polymers and Sequential Copolymers by Polyfunctional Initiator-Transfer Agents (Inifers) - III. Synthesis and Characterization of Poly( $\alpha$ -Methylstyrene-B-Isobutylene-B- $\alpha$ -Methylstyrene). *J. Polym. Sci. Polym. Chem. Ed.* **1980**, *18*, 1539–1546.
- (10) Kennedy, J. P.; Puskas, J. E.; Kaszas, G.; Hager, W. G. Thermoplastic Elastomers



- of Isobutylene and Process of Preparation. US Patent 4,946,899, 1990.
- (11) Kaszas, G.; Puskas, J. E.; Kennedy, J. P. Polyisobutylene-Containing Block Polymers by Sequential Monomer Addition. II. Polystyrene–polyisobutylene–polystyrene Triblock Polymers: Synthesis, Characterization, and Physical Properties. *J. Polym. Sci. Part A Polym. Chem.* **1991**, *29* (3), 427–435.
  - (12) Kennedy, J. P. From Thermoplastic Elastomers to Designed Biomaterials. *J. Polym. Sci. Part A Polym. Chem.* **2005**, *43* (14), 2951–2963.
  - (13) Zaszke, B.; Kennedy, J. P. Novel Thermoplastic Elastomers: Polyisobutylene-Block-Polyamide Multiblocks. *Macromolecules* **1995**, *28* (13), 4426–4432.
  - (14) Kucera, L. R.; Brei, M. R.; Storey, R. F. Synthesis and Characterization of Polyisobutylene-B-Polyamide Multi-Block Copolymer Thermoplastic Elastomers. *Polymer (Guildf)*. **2013**, *54* (15), 3796–3805.
  - (15) Kucera, L. R. Synthesis and Characterization of Polyisobutylene-Block-Polyamides as Novel Thermoplastic Elastomers, University of Southern Mississippi, 2013.
  - (16) Odian, G. *Principles of Polymerization*, 4th ed.; John Wiley & Sons, Inc.: Hoboken, 2004.
  - (17) *Characterization and Failure Analysis of Plastics*; ASM International: Materials Park, OH, 2003.
  - (18) Storey, R. F.; Choate, K. R. Kinetic Investigation of the Living Cationic Polymerization of Isobutylene Using a T-Bu-M-DCC/TiCl<sub>4</sub>/2,4-DMP Initiating System. *Macromolecules* **1997**, *30* (96), 4799–4806.
  - (19) Barrère, C.; Hubert-Roux, M.; Lange, C. M.; Rejaibi, M.; Kebir, N.; Désilles, N.;

- Lecamp, L.; Burel, F.; Loutelier-Bourhis, C. Solvent-Based and Solvent-Free Characterization of Low Solubility and Low Molecular Weight Polyamides by Mass Spectrometry: A Complementary Approach. *Rapid Commun. Mass Spectrom.* **2012**, *26* (11), 1347–1354.
- (20) Zhang, C.; Feng, L.; Gu, X.; Hoppe, S.; Hu, G.-H. Determination of the Molar Mass of Polyamide Block/graft Copolymers by Size-Exclusion Chromatography at Room Temperature. *Polym. Test.* **2007**, *26*, 793–802.
- (21) American Polymer Standards Corporation. Light Scattering dn/dc Values <http://www.ampolymer.com/dn-dcValues.html>.
- (22) ASTM Standard D 638, Standard Test Method for Tensile Properties of Plastics. **1994**.
- (23) ASTM Standard D 412, Standard Test Methods for Vulcanized Rubber and Thermoplastic Rubbers and Thermoplastic Elastomers--Tension. **1994**.
- (24) Liu, T.; Petermann, J. Multiple Melting Behavior in Isothermally Cold-Crystallized Isotactic Polystyrene. *Polymer (Guildf)*. **2001**, *42* (15), 6453–6461.
- (25) Richards, R. B. Polyethylene - Structure, Crystallinity, and Properties. *J. Appl. Chem.* **1951**.
- (26) Medellín-Rodríguez, F. J.; Larios-López, L.; Zapata-Espinoza, A.; Dávalos-Montoya, O.; Phillips, P. J.; Lin, J. S. Melting Behavior of Polymorphics: Molecular Weight Dependence and Steplike Mechanisms in Nylon-6. *Macromolecules* **2004**, *37* (5), 1799–1809.
- (27) INVISTA. *Technical Bulletin: The Difference between Type 6,6 and Type 6 Nylon*; 2013.

- (28) *Nylon Plastics Handbook*; Kohan, M. I., Ed.; Munich, 1995.
- (29) Yang, B.; Parada, C. M.; Storey, R. F. Synthesis, Characterization, and Photopolymerization of Polyisobutylene Phenol (Meth)acrylate Macromers. *Macromolecules* **2016**, *49* (17), 6173–6185.
- (30) Ojha, U.; Kulkarni, P.; Faust, R. Syntheses and Characterization of Novel Biostable Polyisobutylene Based Thermoplastic Polyurethanes. *Polymer (Guildf)*. **2009**, *50* (15), 3448–3457.

